

See discussions, stats, and author profiles for this publication at: <https://www.researchgate.net/publication/231432187>

Syntheses of Macrocyclic Enzyme Models. 8. Conformational Mobility and Molecular Recognition by the Internal Cage of Kyuphane

ARTICLE *in* JOURNAL OF THE AMERICAN CHEMICAL SOCIETY · OCTOBER 1991

Impact Factor: 12.11 · DOI: 10.1021/ja00022a006

CITATIONS

36

READS

11

8 AUTHORS, INCLUDING:



Teruhisa Ohno

Kyushu Institute of Technology

164 PUBLICATIONS 5,977 CITATIONS

SEE PROFILE



Yoshio Hisaeda

Kyushu University

250 PUBLICATIONS 3,726 CITATIONS

SEE PROFILE

Syntheses of Macrocyclic Enzyme Models. 8.[†] Conformational Mobility and Molecular Recognition by the Internal Cage of Kyuphane

Yukito Murakami,^{*,‡} Jun-ichi Kikuchi,^{‡,§} Teruhisa Ohno,[‡] Takayuki Hirayama,[‡]
Yoshio Hisaeda,[‡] Hiroshi Nishimura,[‡] James P. Snyder,^{*,⊥} and Kosta Steliou^{||}

Contribution from the Department of Organic Synthesis, Faculty of Engineering, Kyushu University, Fukuoka 812, Japan, Searle Research and Development, Skokie, Illinois 60077, and the Department of Chemistry, University of Montreal, Montreal, Quebec, Canada H3C 3V1. Received February 1, 1991

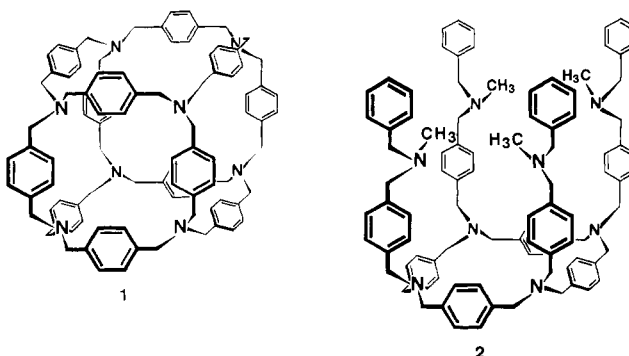
Abstract: Temperature-dependent ¹H NMR measurements in CDCl₃-CS₂ (3:7 v/v) and DMF-*d*₇ in concert with MM2 conformational analysis reveal that the molecular framework of "Kyuphane" (**1**), a cage-type cubical molecule with six faces each consisting of a 2,11,20,29-tetraaza[3.3.3.3]paracyclophane ring, is significantly more rigid than the corresponding noncage host (**2**), but still conformationally flexible. A slow rate of interconversion among degenerated conformers of the lowest energy C₂ conformation accounts for the observed NMR line broadening. Hosts **1** and **2** are soluble in acidic aqueous media below pH 4 and behave as polycationic species. Electrostatic field solvation analysis of the tetraprotonated salt of Kyuphane suggests a square-planar proton placement (**11a**) to predominate in solution. Line broadening for the tetracation appears to arise from both conformer interconversion and proton exchange. Guest recognition behavior of these hosts under acidic conditions was studied by means of ¹H NMR and fluorescence spectroscopy. Kyuphane demonstrates a pH-dependent guest-binding ability due to changes in the specific microenvironmental polarity of its three-dimensional cavity upon variable protonation of the nitrogen atoms. The host also shows size-sensitive and regioselective molecular discrimination originating from the semirigid geometry of the hydrophobic cavity and the specific protonation geometry. The specific molecular discrimination evidenced by **1** was analyzed by MM2 molecular mechanics and applied to selective transport of hydrophobic molecules between organic phases across an aqueous phase in which **1** was present as a carrier. It is noteworthy that the proton NMR signals of guest molecules naphthalene-2,6-disulfonate, 8-anilinoanthracene-1-sulfonate, and 6-*p*-toluidinonaphthalene-2-sulfonate completely disappear upon complexation with Kyuphane, whereas the identical guest naphthalene-2,6-disulfonate shows normal upfield shifts of its NMR proton signals upon complexation with **2**.

Introduction

The development of artificial hosts exhibiting potent recognition capabilities toward guest molecules is of great importance for creating supramolecules such as artificial carriers, enzymes, and receptors. Macrocyclic compounds having a sizeable internal cavity exemplify the formation of supramolecular assemblies. Modifications of the internal cavities can result in specific guest-binding modes.¹⁻⁶ Cyclophane hosts capable of providing a three dimensionally extended hydrophobic cavity have been shown to perform guest recognition superior to the corresponding untethered macrocycles. For instance, we have shown that octopus cyclophanes constructed with a cyclophane ring and eight flexible hydrophobic branches exercise guest recognition most likely by an induced-fit phenomenon in aqueous media.⁷ On the other hand, cyclophane hosts with condensed macrocycles have been investigated by several research groups.⁸⁻¹⁴ Molecular skeletons of the latter hosts are relatively rigid. Their internal cavities seem to perform host-guest recognition through the lock-and-key mechanism. However, in most cases, the internal cavities are not well shielded from the external solvent medium.

In this context, we now report the preparation and unique guest recognition ability of a novel host (**1**), whose internal cavity is considerably shielded from external aqueous media.¹⁵ Host **1** furnishes a relatively rigid and large hydrophobic cavity surrounded by six faces each consisting of a 2,11,20,29-tetraaza[3.3.3.3]paracyclophane ring. We propose the abbreviated name "Kyuphane" (Kyushu + cyclophane) for this host after its birthplace. The corresponding noncage host (**2**) has also been synthesized as a reference with which to contrast the specific

molecular recognition features of **1**. Organic guest molecules used in this work are summarized in Chart I.



- (1) Tabushi, I.; Yamamura, K. *Top. Curr. Chem.* **1983**, *113*, 145-185.
- (2) (a) Murakami, Y. *Top. Curr. Chem.* **1983**, *115*, 107-155. (b) Murakami, Y. *J. Inclusion Phenom.* **1984**, *2*, 35-47. (c) Murakami, Y.; Kikuchi, J. *Pure Appl. Chem.* **1988**, *60*, 549-554.
- (3) Odashima, K.; Koga, K. In *Cyclophanes*; Keehn, P. M.; Rosenfeld, S. M., Eds.; Academic Press: New York, 1983; Vol. 2, Chapter 11.
- (4) Diederich, F. *Angew. Chem., Int. Ed. Engl.* **1988**, *27*, 362-386.
- (5) (a) Bender, M. L.; Komiya, M. *Cyclodextrin Chemistry*; Springer: Berlin, 1978. (b) D'Souza, V. T.; Bender, M. L. *Acc. Chem. Res.* **1987**, *20*, 146-158.
- (6) (a) Breslow, R. *Science (Washington, D.C.)* **1982**, *218*, 532-537. (b) Breslow, R. *Adv. Enzymol. Relat. Areas Mol. Biol.* **1986**, *58*, 1-60.
- (7) (a) Murakami, Y.; Kikuchi, J.; Suzuki, M.; Matsuura, T. *J. Chem. Soc., Perkin Trans. 1* **1988**, 1289-1299. (b) Murakami, Y.; Kikuchi, J.; Ohno, T.; Hayashida, O.; Kojima, M. *J. Am. Chem. Soc.* **1990**, *112*, 7672-7681.
- (8) (a) Diederich, F.; Dick, K. *Angew. Chem., Int. Ed. Engl.* **1984**, *23*, 810-812. (b) Diederich, F.; Dick, K.; Griebel, D. *J. Am. Chem. Soc.* **1986**, *108*, 2273-2286.
- (9) (a) Miller, S. P.; Whitlock, H. W., Jr. *J. Am. Chem. Soc.* **1984**, *106*, 1492-1494. (b) Sheridan, R. E.; Whitlock, H. W., Jr. *J. Am. Chem. Soc.* **1986**, *108*, 7020-7021.
- (10) Murakami, Y.; Kikuchi, J.; Tenma, H. *J. Chem. Soc., Chem. Commun.* **1985**, 753-755.

[†] Part 7: see ref 7b.

[‡] Kyushu University.

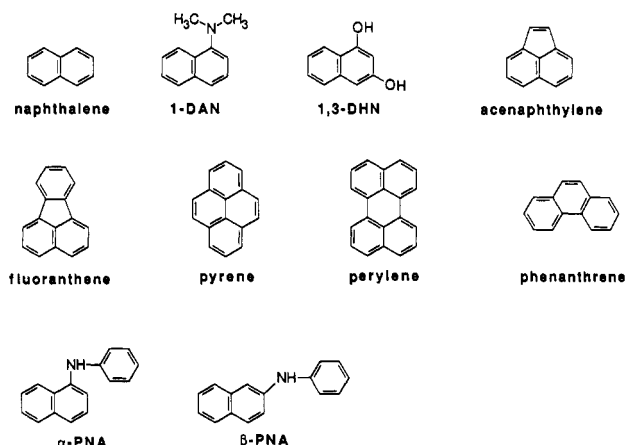
[§] Present address: Department of Applied Chemistry, Faculty of Science and Engineering, Saga University, Saga 840, Japan.

[⊥] Inquiries regarding computational aspects of the work should be addressed to this author at Searle Research and Development.

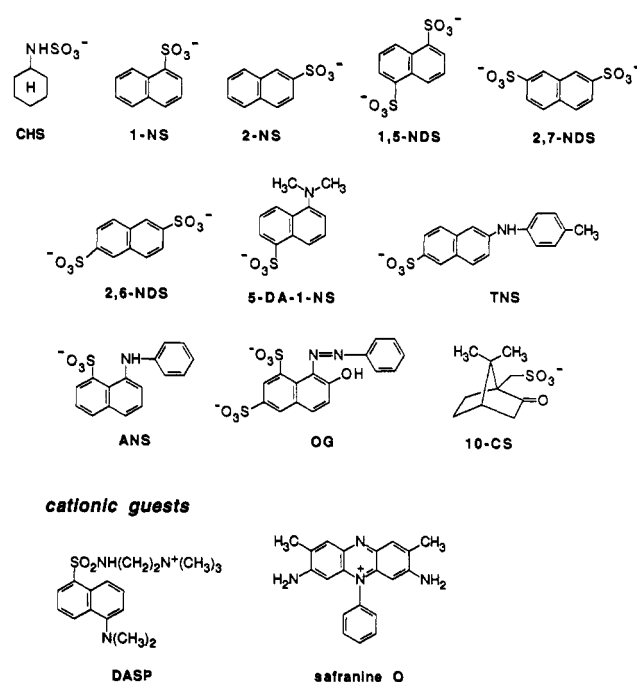
^{||} University of Montreal.

Chart I

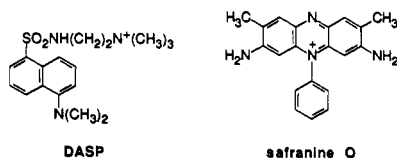
nonionic guests



anionic guests

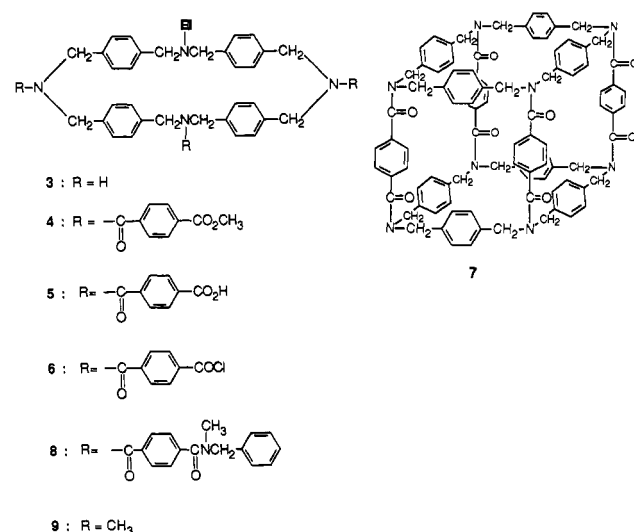


cationic guests



The unique and topologically cubical structure of **1** raises a number of questions. Obviously more rigid than the uncapped species **2**, does Kyuphane support a complex conformational potential energy surface? The six somewhat flexible faces are entry channels into the charge-lined central cavity for guests. Can specific features of guest geometry be correlated with relative selectivity and binding ability? At pH 4.0, host **1** exists as an NH^+ tetracation able to complex both nonionic and anionic

guests.^{15a,b} Which of several protonation schemes are energetically accessible to the Kyuphane multiple salt? An array of spectroscopic and theoretical methods employed to answer these and related questions leads to a sketch of Kyuphane as a basic, semi-rigid, dynamic molecule capable of showing a variety of complexation modes.



Experimental Section

Guest Compounds. The following compounds were obtained from commercial sources as guaranteed reagents and used without further purification: magnesium bis(8-anilidonaphthalene-1-sulfonate) [$\text{Mg}(\text{ANS})_2$], potassium 6-*p*-toluidinonaphthalene-2-sulfonate [$\text{K}(\text{TNS})$], [[1-(dimethylamino)naphthalene-5-sulfonamido]ethyl]trimethylammonium perchlorate [(DASP) ClO_4], disodium naphthalene-2,6-disulfonate [$\text{Na}_2(2,6\text{-NDS})$], naphthalene-1-sulfonic acid [$\text{H}(1\text{-NS})$], naphthalene-2-sulfonic acid [$\text{H}(2\text{-NS})$], naphthalene, and phenanthrene (these from Nacalai Tesque, Inc., Kyoto, Japan); 5-(dimethylamino)naphthalene-1-sulfonic acid [$\text{H}(5\text{-DA-1-NS})$], disodium naphthalene-1,5-disulfonate [$\text{Na}_2(1,5\text{-NDS})$], disodium naphthalene-2,7-disulfonate [$\text{Na}_2(2,7\text{-NDS})$], 1-(dimethylamino)naphthalene (1-DAN), 1,3-dihydroxynaphthalene (1,3-DHN), and fluorenone (these from Tokyo Kasei Kogyo Co., Tokyo, Japan); sodium *N*-cyclohexylsulfamate [$\text{Na}(\text{CHS})$] and acenaphthylene (both from Ishizu Seiyaku Co., Osaka, Japan); Orange G (disodium 7-hydroxy-8-phenylazonaphthalene-1,3-disulfonate) [$\text{Na}_2(\text{OG})$]; Wako Pure Chemical Industries, Osaka, Japan]; (\pm)-10-camphorsulfonic acid [$\text{H}(10\text{-CS})$]; Aldrich Chemical Co., Inc., Milwaukee, WI]; and safranin O (3,7-diamino-2,8-dimethyl-5-phenylphenazinium chloride) (Chroma Gesellschaft, König, FRG). Pyrene (Nacalai Tesque) was purified by means of liquid chromatography on a column of silica gel (Wako Gel C-100) with cyclohexane as eluent;¹⁶ mp 149–151 °C. *N*-Phenyl-1-naphthylamine (α -PNA), *N*-phenyl-2-naphthylamine (β -PNA), and perylene (these from Tokyo Kasei Kogyo) were recrystallized from methanol–water (4:1 v/v) (mp 60–61 °C), methanol–water (5:1 v/v) (mp 108–109 °C), and acetone–water (1:1 v/v) (mp 278–279 °C), respectively.

***p*-Bis[(trifluoroacetyl)amino]methylbenzene.** Trifluoroacetic anhydride (50 mL, 0.35 mol) was added dropwise in 85 min to a mixture of *p*-xylylenediamine (22.0 g, 0.16 mol) and dry diethyl ether (350 mL) with vigorous stirring at 0 °C, and the mixture was stirred further for 1 day at room temperature. Insoluble materials were collected by filtration and recrystallized from acetone–dichloromethane (3:1 v/v) to give white needles (37.1 g, 70.6%); mp 199.0–201.5 °C; TLC R_f (Wako Silica Gel 70FM; ethyl acetate) 0.86; IR (KBr disc) 1700 (C=O) and 1190 (CF) cm^{-1} ; ^1H NMR (60 MHz, CDCl_3 - $\text{DMSO}-d_6$ (1:2 v/v), 308 K) δ 4.34 (4 H, d, CH_2), 7.19 (4 H, s, phenyl protons), and 9.70 (2 H, t, NH).

2,11,20,29-Tetraaza[3.3.3.3]paracyclophane (3). A solution of *p*-bis[(trifluoroacetyl)amino]methylbenzene (16.4 g, 50 mmol) in dry *N,N*-dimethylformamide (DMF) (50 mL) was added dropwise in 15 min to a mixture of sodium hydride (60% dispersion in mineral oil; 5.0 g, 125 mmol) and dry DMF (400 mL) with stirring under nitrogen at room temperature, and the mixture was stirred for 10 min more. A solution of *p*-xylylenedichloride (8.8 g, 50 mmol) in dry DMF (250 mL) was added to the resulting mixture with vigorous stirring in 2 h at 60 °C, and

(11) (a) Franke, J.; Vögtle, F. *Angew. Chem., Int. Ed. Engl.* **1985**, *24*, 219–221. (b) Wambach, L.; Vögtle, F. *Tetrahedron Lett.* **1985**, *26*, 1483–1486. (c) Merz, T.; Wirtz, H.; Vögtle, F. *Angew. Chem., Int. Ed. Engl.* **1986**, *25*, 567–569. (d) Vögtle, F.; Müller, W. M.; Werner, U.; Losensky, H.-W. *Angew. Chem., Int. Ed. Engl.* **1987**, *26*, 901–903.

(12) O'Krongly, D.; Denmeade, S. R.; Chiang, M. Y.; Breslow, R. *J. Am. Chem. Soc.* **1985**, *107*, 5544–5545.

(13) Cancelli, J.; Lacombe, L.; Collet, A. *J. Am. Chem. Soc.* **1986**, *108*, 4230–4232.

(14) Cram, D. J.; Karbach, S.; Kim, Y. H.; Baczyński, L.; Marti, K.; Sampson, R. M.; Kallemeyn, G. W. *J. Am. Chem. Soc.* **1988**, *110*, 2554–2560.

(15) Preliminary reports: (a) Murakami, Y.; Kikuchi, J.; Hirayama, T. *Chem. Lett.* **1987**, 161–164. (b) Murakami, Y.; Kikuchi, J.; Ohno, T.; Hirayama, T. *Chem. Lett.* **1989**, 881–884. (c) Murakami, Y.; Kikuchi, J.; Ohno, T.; Hirayama, T.; Nishimura, H. *Chem. Lett.* **1989**, 1199–1202.

(16) Kano, K.; Takenoshita, I.; Ogawa, T. *J. Phys. Chem.* **1982**, *86*, 1833–1838.

the mixture was stirred for 6 h more at the same temperature. The hot mixture was filtered, and the filtrate was evaporated to dryness to give a yellow solid (22.6 g). Then, a mixture of the solid (11.0 g), sodium tetrahydroborate (4.4 g, 126 mmol), and ethanol (180 mL) was refluxed with stirring for 2.5 h. The hot mixture was filtered, and water (260 mL) was added to the filtrate. The pH of the solution was adjusted to 1 by adding concentrated hydrochloric acid, ethanol was evaporated off, and aqueous ammonia was added to the residue to retain its pH at 13. The resulting water-insoluble material was extracted with benzene (5 × 100 mL), water was removed from the benzene extract by treatment with silicone-treated filter paper (Whatman 1PS), and the solvent was evaporated under reduced pressure. The crude product was purified by gel filtration chromatography on a column of Sephadex LH-20 with methanol-chloroform (1:1 v/v) as eluant. Evaporation of the solvent under reduced pressure gave a colorless solid (973 mg, 17%); mp 140 °C; IR (KBr disc) 3270 (NH) cm^{-1} ; ^1H NMR (400 MHz, CDCl_3 , 291 K) δ 1.65 (4 H, s, NH), 3.64 (16 H, s, CH_2), and 6.90 (16 H, s, phenyl protons); ^{13}C NMR (100 MHz, CDCl_3 , 303 K) δ 52.72 (CH_2), 128.35 (C-2, C-3, C-5, and C-6 of phenyl carbons), and 139.19 (C-1 and C-4 of phenyl carbons); mass spectrum (EI-MS), m/e 476 (M^+); calcd MW for $\text{C}_{32}\text{H}_{36}\text{N}_4$, 476. Anal. Calcd for $\text{C}_{32}\text{H}_{36}\text{N}_4 \cdot \frac{1}{2}\text{H}_2\text{O}$: C, 79.14; H, 7.68; N, 11.54. Found: C, 79.29; H, 7.73; N, 11.12.

***N,N',N'',N'''*-Tetrakis[4-(methoxycarbonyl)benzoyl]-2,11,20,29-tetraaza[3.3.3.3]paracyclophane (4).** A solution of compound 3 (1.12 g, 2.35 mmol) in dry dichloromethane (80 mL) was added dropwise in 20 min to a mixture of methyl 4-(chloroformyl)benzoate (3.3 g, 16.5 mmol) and triethylamine (2.4 mL, 17.0 mmol) in dry dichloromethane (80 mL) with stirring at room temperature. The resulting mixture was stirred for 1 day at the same temperature. It was then evaporated to dryness under reduced pressure, and the residue was purified by gel filtration chromatography on a column of Sephadex LH-20 with methanol-chloroform (1:1 v/v) as eluant. Evaporation of the solvent under reduced pressure gave a white solid (2.35 g, 89%), mp 147–148.5 °C. Purification of the product by liquid chromatography on a column of silica gel (Wakogel C-300) with dichloromethane-acetone (10:1 v/v) was also applicable (61%). This method is more suitable for purification on a large scale than the former: IR (KBr disc) 1725 and 1637 ($\text{C}=\text{O}$) cm^{-1} ; ^1H NMR (400 MHz, CDCl_3 , 291 K) δ 3.92 (12 H, s, CH_3), 4.53 (16 H, m, CH_2), 6.95 (16 H, m, CH_2Ar phenyl protons), 7.54 (8 H, br s, H-2 and H-6 of COAr phenyl protons), and 8.08 (8 H, br s, H-3 and H-5 of COAr phenyl protons); ^{13}C NMR (100 MHz, CDCl_3 , 303 K) δ 48.37 and 52.93 (CH_2), 52.29 (CH_3), 126.67 (C-2 and C-6 of COAr phenyl carbons), 127.52 and 128.81 (C-2, C-3, C-5, and C-6 of CH_2Ar phenyl carbons), 129.93 (C-4 of COAr phenyl carbons), 131.24 (C-1 of COAr phenyl carbons), 135.33 and 135.53 (C-1 and C-4 of CH_2Ar phenyl carbons), 140.28 (C-3 and C-5 of COAr phenyl carbons), 166.16 (NCO), and 171.07 (CO_2CH_3); mass spectrum (FD-MS), m/e 1124 (M^+); calcd MW for $\text{C}_{68}\text{H}_{60}\text{N}_4\text{O}_{12}$, 1124. Anal. Calcd for $\text{C}_{68}\text{H}_{60}\text{N}_4\text{O}_{12} \cdot \frac{3}{2}\text{H}_2\text{O}$: C, 70.88; H, 5.51; N, 4.86. Found: C, 70.83; H, 5.22; N, 4.77.

***N,N',N'',N'''*-Tetrakis(4-carboxybenzoyl)-2,11,20,29-tetraaza[3.3.3.3]paracyclophane (5).** A mixture of 4 (1.18 g, 1.05 mmol), aqueous sodium hydroxide (1 M; 47 mL), and ethanol (200 mL) was refluxed for 16 h and cooled to room temperature. Ethanol was evaporated off under reduced pressure, and water (50 mL) was added to the residue. The pH of the solution was adjusted to 2 by adding aqueous hydrochloric acid (2 M) after removal of a small amount of insoluble materials by filtration, and the solution was allowed to stand overnight at 5 °C. Precipitates were recovered, washed with water, and purified by gel filtration chromatography on a column of Sephadex LH-20 with methanol-chloroform (1:1 v/v) as eluant. Evaporation of the solvent under reduced pressure gave a colorless solid (1.04 g, 93%); mp 239.0–240.0 °C; IR (KBr disc) 1725 and 1620 ($\text{C}=\text{O}$) cm^{-1} ; ^1H NMR (400 MHz, $\text{CD}_3\text{OD}-\text{CDCl}_3$ (1:1 v/v), 303 K) δ 4.57 (16 H, m, CH_2), 6.99 (16 H, m, CH_2Ar phenyl protons), 7.56 (8 H, br s, H-2 and H-6 of COAr phenyl protons), and 8.11 (8 H, br s, H-3 and H-5 of COAr phenyl protons); ^{13}C NMR (100 MHz, $\text{CD}_3\text{OD}-\text{CDCl}_3$ (1:1 v/v), 303 K) δ 52.70 (CH_2), 125.92 (C-2 and C-6 of COAr phenyl carbons), 127.09 and 128.61 (C-2, C-3, C-5, and C-6 of CH_2Ar phenyl carbons), 129.61 (C-4 of COAr phenyl carbons), 132.01 (C-1 of COAr phenyl carbons), 134.83 and 135.79 (C-1 and C-4 of CH_2Ar phenyl carbons), 139.20 (C-3 and C-5 of COAr phenyl carbons), 167.59 (NCO), and 171.47 (CO_2H); mass spectrum (FAB-MS), m/e 1069 ($\text{M}^+ + \text{H}$); calcd MW for $\text{C}_{64}\text{H}_{52}\text{N}_4\text{O}_{12}$, 1069 ($\text{M}^+ + \text{H}$). Anal. Calcd for $\text{C}_{64}\text{H}_{52}\text{N}_4\text{O}_{12} \cdot 2\text{H}_2\text{O}$: C, 69.56; H, 5.11; N, 5.07. Found: C, 69.53; H, 4.99; N, 4.98.

Precursor of Kyuphane (7). A mixture of 5 (650 mg, 608 μmol) and thionyl chloride (25 mL, 125 mmol) was stirred for 14 h at room temperature. The excess thionyl chloride was removed under reduced pressure, and a small amount of dry dichloromethane was added to the residue with stirring. The solvent was evaporated off under reduced pressure to give the acid chloride 6 quantitatively. Solutions of 3 (290

mg, 608 μmol) and 6 (695 mg, 608 μmol) in dry dichloromethane-benzene (150:7 v/v; 200 mL each) were added dropwise over 11 h to a solution of triethylamine (0.5 g, 5 mmol) in dry dichloromethane-benzene (150:7 v/v; 1570 mL) at an identical rate with vigorous stirring under nitrogen at room temperature, and the mixture was stirred for 12 h more. The reaction mixture was evaporated to dryness under reduced pressure, and 25 mL of methanol-chloroform (1:1 v/v) was added to the residue. The mixture was evaporated to dryness after removal of insoluble materials by filtration, and the residue was purified by gel filtration chromatography on a column of Toyopearl HW-40 fine with methanol-chloroform (1:1 v/v) as eluant. Evaporation of the solvent under reduced pressure gave a colorless solid (34 mg, 3.8%); mp 350 °C (dec); IR (KBr disc) 1630 ($\text{C}=\text{O}$) cm^{-1} ; ^1H NMR (400 MHz, CDCl_3 , 291 K) δ 2.9–5.5 (32 H, m, CH_2), and 5.5–8.2 (32 H, m, phenyl protons); ^{13}C NMR (100 MHz, CDCl_3 , 303 K) δ 40–60 (CH_2), 123–133 (C-2 and C-3 of phenyl carbons), 133–142 (C-1 and C-4 of phenyl carbons), and 167–174 (CO). Anal. Calcd for $\text{C}_{96}\text{H}_{80}\text{N}_8\text{O}_8 \cdot 4\text{H}_2\text{O}$: C, 74.59; H, 5.73; N, 7.24. Found: C, 74.74; H, 5.57; N, 7.14.

Kyuphane (1). A solution of 7 (39 mg, 26 μmol) in dry dichloromethane (20 mL) was stirred at room temperature under nitrogen atmosphere for 1 h. Borane-dimethyl sulfide (borane content 10 M; 3 mL, 30 mmol) was added to the solution, and the mixture was stirred for 1 h more under nitrogen atmosphere. The dissociated dimethyl sulfide was distilled off, and the mixture was refluxed for 7 h under nitrogen atmosphere. Then, the solvent was evaporated under reduced pressure, aqueous hydrochloric acid (4 M; 12 mL) was added to the residue, and the mixture was refluxed for 1 h. The reaction mixture was cooled to room temperature, and water (100 mL) was added to it. After removal of a small amount of insoluble materials by filtration (glass filter G3), the pH of the aqueous solution on an ice bath was adjusted to 12 by adding dilute aqueous sodium hydroxide. The resulting precipitates were recovered, washed with water, and dried under reduced pressure at room temperature to give a pale brown solid, which was subsequently dissolved in benzene (10 mL). After removal of a small amount of insoluble materials by filtration, the solvent was evaporated off under reduced pressure, and the residue was dried at 25 °C (0.015 mmHg) for 6 h to give a white solid [1-benzene (1:1) complex]. The complex was dissolved in a small amount of benzene, and a large amount of methanol was added to it. The solvent was evaporated under reduced pressure, and the residue was dried at 64.5 °C (0.003 mmHg) for 24 h to give 1, free from solvent molecules, as a white solid (33 mg, 93%); mp 202 °C (dec); ^1H NMR (400 MHz, CDCl_3 , 303 K) δ 2.8–4.3 (48 H, m, CH_2), and 6.6–8.1 (48 H, m, phenyl protons); ^{13}C NMR (100 MHz, CDCl_3 , 303 K) δ 57–59 (CH_2), 127–130 (C-2 and C-3 of phenyl carbons), and 138–140 (C-1 and C-4 of phenyl carbons); mass spectrum (FAB-MS), m/e 1362 ($\text{M}^+ + \text{H}$); calcd MW for $\text{C}_{96}\text{H}_{96}\text{N}_8$, 1362 ($\text{M}^+ + \text{H}$). Anal. Calcd for $\text{C}_{96}\text{H}_{96}\text{N}_8 \cdot \frac{3}{2}\text{H}_2\text{O}$: C, 81.96; H, 7.09; N, 7.96. Found: C, 82.00; H, 7.24; N, 7.77.

***N,N',N'',N'''*-Tetrakis[4-(*N*-benzyl-*N*-methylcarbamoyl)benzoyl]-2,11,20,29-tetraaza[3.3.3.3]paracyclophane (8).** The acid chloride 6 was prepared by the reaction of 5 (100 mg, 90 μmol) with thionyl chloride (8 mL, 40 mmol) in a manner similar to that stated above for the synthesis of 7. A solution of 6 (90 μmol) in dry dichloromethane (15 mL) was added dropwise to a mixture of *N*-methylbenzylamine (90 mg, 740 μmol) and triethylamine (0.54 g, 5.3 mmol) in dry dichloromethane (15 mL) at room temperature with stirring. Stirring was continued for 1 day at room temperature. The solvent was removed under reduced pressure, and the residue was purified by gel filtration chromatography on a column of Sephadex LH-20 with methanol-chloroform (1:1 v/v) as eluant. Evaporation of the solvent under reduced pressure gave a colorless solid (104 mg, 75%); mp 143–144 °C; IR (KBr disc) 1640 ($\text{C}=\text{O}$) cm^{-1} ; ^1H NMR (400 MHz, CDCl_3 , 303 K) δ 2.95 (12 H, d, CH_3), 4.55 (24 H, m, CH_2), 6.98 (16 H, m, CH_2ArCH_2 phenyl protons), 7.31 [20 H, m, $\text{CON}(\text{CH}_3)\text{CH}_2\text{Ar}$ phenyl protons], and 7.49 (16 H, br s, COAr phenyl protons); ^{13}C NMR (100 MHz, CDCl_3 , 303 K) δ 33.25 and 36.88 (CH_3), 48.04 and 52.96 (CH_2NCH_2), 50.80 and 55.03 [$\text{N}(\text{CH}_3)\text{CH}_2\text{Ar}$], 126.5–129.1 [C-2, C-3, C-5, and C-6 of CH_2ArCH_2 phenyl carbons; C-2, C-3, C-5, and C-6 of COArCO phenyl carbons; $\text{N}(\text{CH}_3)\text{CH}_2\text{Ar}$ phenyl carbons], and 135.3–137.6 (C-1 and C-4 of CH_2ArCH_2 phenyl carbons; C-1 and C-4 of COArCO phenyl carbons); mass spectrum (FD-MS), m/e 1481 (M^+); calcd MW for $\text{C}_{96}\text{H}_{88}\text{N}_8\text{O}_8$, 1481 (M^+). Anal. Calcd for $\text{C}_{96}\text{H}_{88}\text{N}_8\text{O}_8 \cdot 2\text{H}_2\text{O}$: C, 75.97; H, 6.11; N, 7.38. Found: C, 75.85; H, 5.85; N, 7.28.

***N,N',N'',N'''*-Tetrakis[4-(*N*-benzyl-*N*-methylamino)methyl]benzyl]-2,11,20,29-tetraaza[3.3.3.3]paracyclophane (2).** A solution of 8 (60 mg, 40 μmol) in dry tetrahydrofuran (20 mL) was stirred for 1 h at room temperature under nitrogen atmosphere. Borane-dimethyl sulfide (borane content 10 M; 3 mL, 30 mmol) was added to the solution, and the mixture was stirred for 1 h under nitrogen atmosphere. The dissociated dimethyl sulfide was distilled off, and the mixture was refluxed for 6 h

under nitrogen atmosphere. Then, the solvent was evaporated off under reduced pressure, aqueous hydrochloric acid (4 M; 24 mL) was added to the residue, and the mixture was refluxed for 1 h. The reaction mixture was cooled to room temperature, and water (100 mL) was added to it. After removal of a small amount of insoluble materials by filtration (glass filter G3), the pH of the aqueous solution placed on an ice bath was adjusted to 10 by adding dilute aqueous sodium hydroxide. The resulting precipitates were recovered, washed with water, and dried under reduced pressure at room temperature to give **2** as the heptahydrochloride salt, a colorless solid (25 mg, 46%); mp 196 °C (dec); ^1H NMR (400 MHz, CDCl_3 , 303 K) δ 2.19 (12 H, s, CH_3), 3.41 [16 H, s, $\text{CH}_2\text{NCH}_2\text{ArCH}_2\text{N}(\text{CH}_3)\text{CH}_2\text{Ar}$], 3.56 [24 H, m, $\text{CH}_2\text{ArCH}_2\text{N}(\text{CH}_3)\text{CH}_2\text{Ar}$], and 7.23–7.38 (52 H, m, phenyl protons); mass spectrum (SI-MS), m/e 1370 ($\text{M}^+ + \text{H}$); calcd MW for $\text{C}_{96}\text{H}_{104}\text{N}_8$, 1370 ($\text{M}^+ + \text{H}$). Anal. Calcd for $\text{C}_{96}\text{H}_{104}\text{N}_8 \cdot 7\text{HCl} \cdot 3\text{H}_2\text{O}$: C, 68.67; H, 7.02; N, 6.67. Found: C, 68.94; H, 7.31; N, 6.74.

***N,N',N'',N'''*-Tetramethyl-2,11,20,29-tetraaza[3.3.3.3]paracyclophane (9).** This compound was prepared in the following manner analogous to that reported in literature.¹⁷ A mixture of **3** (106 mg, 0.22 mol), 95% formic acid (10 mL), and 37% aqueous formaldehyde (5 mL) was refluxed for 20 h with stirring. Concentrated hydrochloric acid (2.5 mL) was added to the hot mixture, and the mixture was refluxed for 22 h. Water (50 mL) was added to the mixture, which was cooled to room temperature in advance. The pH of the solution was adjusted to 11 by adding 10% aqueous sodium hydroxide, and the resulting insoluble material was extracted with benzene (3 \times 50 mL). The aqueous layer was removed by treatment with silicon-treated filter paper (Whatman 1PS), and the solvent was evaporated under reduced pressure. The crude product was purified by gel filtration chromatography on a column of Sephadex LH-20 with methanol as eluant. Evaporation of the solvent under reduced pressure gave a colorless solid (114 mg, 97%); mp 194.8–195.7 °C; ^1H NMR (400 MHz, CDCl_3 , 298 K) δ 2.33 (12 H, s, CH_3), 3.33 (16 H, s, CH_2), and 7.26 (16 H, s, phenyl protons). Anal. Calcd for $\text{C}_{36}\text{H}_{44}\text{N}_4$: C, 81.16; H, 8.32; N, 10.52. Found: C, 81.19; H, 8.30; N, 10.67.

Preparation and Characterization of Kyuphane–Solvent Complexes. Kyuphane was solidified from its benzene solution upon evaporation of the solvent and subsequently dried at 25 °C (0.015 mmHg) for 6 h to afford a Kyuphane–benzene (1:1) complex: ^1H NMR (400 MHz, CDCl_3 , 298 K) δ 7.37 (6 H, s, C_6H_6); IR (KBr disc) 680 (C_6H_6) cm^{-1} . Anal. Calcd for $\text{C}_{96}\text{H}_{96}\text{N}_8 \cdot \text{C}_6\text{H}_6 \cdot 4\text{H}_2\text{O}$: C, 81.02; H, 7.33; N, 7.41. Found: C, 81.00; H, 7.07; N, 7.56. The composition of the complex did not undergo any change even after heating at 80 °C (0.015 mmHg) for 6 h.

The Kyuphane–benzene (1:1) complex was solidified from its chloroform solution upon evaporation of the solvent. This treatment was repeated three times, and the solid was subsequently dried at 100 °C (0.5 mmHg) for 4 h to afford a Kyuphane–chloroform (1:1) complex: IR (KBr disc) 760 (CHCl_3) cm^{-1} . Anal. Calcd for $\text{C}_{96}\text{H}_{96}\text{N}_8 \cdot \text{CHCl}_3 \cdot 2\text{H}_2\text{O}$: C, 76.79; H, 6.71; N, 7.39. Found: C, 76.66; H, 6.78; N, 7.34. On the other hand, formation of the inclusion complex of Kyuphane with two chloroform molecules in solution was confirmed on the basis of a molecular weight measurement by osmometry: for $\text{C}_{96}\text{H}_{96}\text{N}_8 \cdot 2\text{HCl}$, 1601.

General Analyses and Measurements. Melting points were measured with a Yanagimoto MP-S1 and a Yanaco MP-500D apparatus (hot plate type). Elemental analyses were performed at the Microanalysis Center of Kyushu University. Molecular weight measurements were performed with a Hitachi Perkin-Elmer 115 vapor pressure osmometer. A JEOL JMS-01SG-2 spectrometer was used for electron impact mass spectroscopy (EI-MS), while a JEOL DX-300 spectrometer was used for field desorption (FD-MS), fast atom bombardment (FAB-MS), and a secondary ion mass spectroscopy (SI-MS). IR spectra were recorded on a JASCO IR-810 spectrophotometer. NMR spectra were taken on a Hitachi R-24B (60 MHz for ^1H) and a JEOL JNM-GSX400 (400 and 100 MHz for ^1H and ^{13}C , respectively) spectrometer installed at the Center of Advanced Instrumental Analysis of Kyushu University. A Beckman Φ 71 pH meter equipped with a Beckman 39505 combined electrode was used for pH measurements after calibration with a combination of appropriate standard aqueous buffers. Potentiometric titrations were performed with a Kyoto Electronics AT-310 automatic titrator. Dynamic light scattering measurements were carried out with a Photol (Otsuka Electronics) DLS-700 (He–Ne laser 632.8 nm) spectrophotometer equipped with a NEC PC-9801 RA personal computer. Electronic absorption spectra were taken on a Hitachi 220A or a Hitachi 340 spectrophotometer. Fluorescence spectra were recorded on a Hitachi 650-60 spectrofluorometer, while fluorescence polarization measurements were carried out with a Union Giken FS-501A spectrophotometer

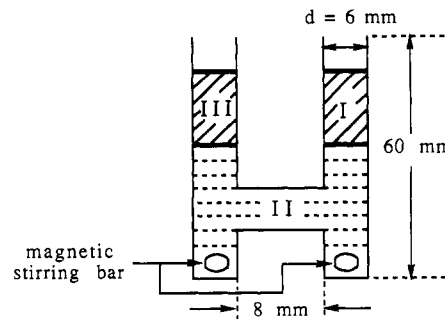


Figure 1. H-type cell used to study the transport of various organic guests.

equipped with a Sord M200 Mark II microcomputer. Fluorescence lifetimes were recorded on a Horiba NAES-1100 time-resolved spectrofluorometer.

Transport Measurements. All measurements were conducted at 25 \pm 1 °C by using an H-type cell shown in Figure 1. The cell was held in exactly the same position relative to a magnetic stirring motor in all measurements. A total of 1000 μL of pure deionized water containing Kyuphane (concentration 1.0×10^{-4} M) was located at the bottom of the cell as phase II. Atop phase II in one arm of the cell, 200 μL of a 4.0×10^{-2} M solution of a guest in hexane was placed as source phase I. In the other arm, 200 μL of hexane was placed atop phase II as receiving phase III. The aqueous phase II was agitated with approximately cylindrical magnetic stirring bars, 3 mm in length and 3 mm in diameter, at a stirring rate to retain clean interfaces between the clear phases. The two arms of the cell were closed with silicone rubber caps during the measurement. Samples were removed from the receiving phase III for determination of amounts of a delivered guest by electronic absorption spectroscopy.

Computational Methods and Application

Three types of molecular manipulations were carried out in the construction of Kyuphane's conformational profile: interactive structure building, geometry optimization, and conformational searching. Both MODEL/BAKMDL¹⁸ and MacroModel/Batchmin¹⁹ equipped with the MM2²⁰ force field were employed for the first two tasks. An efficient Monte Carlo search procedure in MODEL/BAKMDL was used for the latter.²¹ Calculations were performed on a VAX 8650, as were the PRDDO, DelPhi, SYBYL, and molecular volume evaluations described below.

The multitude of potential phenyl–phenyl interactions in **1** was treated by modifying the MM2 force field such that interphenyl $\text{C}_{\text{aro}}\text{--}\text{C}_{\text{aro}}$ van der Waals interactions were set to zero.²² In addition, the $\text{C}_{\text{aro}}\text{--}\text{H}$ and $\text{C}_{\text{aro}}\text{--}\text{C}_{\text{sp}3}$ dipoles were given values of -0.30 . These expedients result in a 0.5–1.0-kcal stabilization for the perpendicular forms of the benzene dimers relative to the parallel form in accord with previous adjustments of the MM2²³ and MM3²⁴ force fields.

Conformational Analysis for Nonionic Kyuphane. Searching the conformational surface of Kyuphane took place in several phases. Initially, we employed a united atom MM2 force field¹⁸ to compensate for the molecule's size: 208 explicit atoms including H's and N lone pairs, 112 without hydrogen. The latter corresponds to structural distortion, geometry optimization, and comparison of the minimized structure with previously found conformations. Though relatively economical, this procedure yielded intermediate united atom structures that were physically unreasonable as a result of strong overemphasis for selected benzene–benzene stackings. The resulting list of structures was nonetheless embellished with hydrogen atoms and reoptimized with the block-diagonal Newton–Raphson procedure in BAKMDL and a final round of full

(18) The current program, derived from an early forerunner of MacroModel, continues to be developed in the laboratory of K. Steliou.

(19) Mohamadi, F.; Richards, N. G. J.; Guida, W. C.; Liskamp, R.; Lipton, M.; Caufield, C.; Chang, G.; Hendrickson, T.; Still, W. C. (MacroModel V2.5) *J. Comput. Chem.* **1990**, *11*, 440–467.

(20) Allinger, N. L. *J. Am. Chem. Soc.* **1977**, *99*, 8127–8134.

(21) Steliou, K. Presented at the 1989 International Chemical Congress of Pacific Basin Societies, Honolulu, Hawaii, December 1989. Steliou, K.; Gajewski, J. J.; Gilbert, K. K.; Midland, M. M.; Tipson, G. E. Manuscript in preparation.

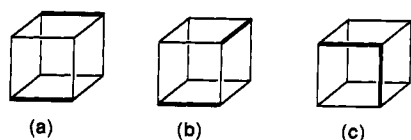
(22) Spangler, D. P.; Steliou, K.; Gajewski, J. J.; Gilbert, K. K. Unpublished work.

(23) Pettersson, I.; Liljefors, T. *J. Comput. Chem.* **1987**, *8*, 1139–1145.

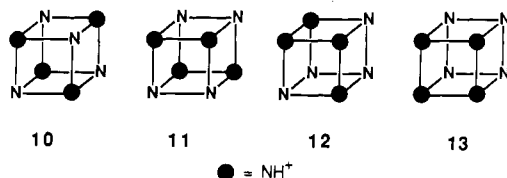
(24) Allinger, N. L.; Lii, J.-H. *J. Comput. Chem.* **1987**, *8*, 1146–1153.

(17) Takemura, H.; Suenaga, M.; Sakai, K.; Kawachi, H.; Shinmyozu, T.; Miyahara, Y.; Inazu, T. *J. Inclusion Phenom.* **1984**, *2*, 207–214.

Scheme I



Scheme II

**Table I.** Relative MM2 (Gas Phase) Energies [$\Delta E_{\text{MM2}}(\text{rel})$] and Percent Populations for Nonionic and Tetracation Kyuphane Conformations (kcal/mol)^{a,b}

	conformation				
	a	b	c	d	e
1	0.0 (91.6)	2.1 (2.8)	2.5 (1.4)	3.6 (0.2)	5.4 (0.01)
10	0.5 (21.2)	0.4 (25.1)	1.5 (3.9)	3.1 (0.3)	3.7 (0.1)
11	0.0 (49.4)	8.5 (0.0)	7.7 (0.0)	6.9 (0.0)	10.3 (0.0)
	10.8 ^c (0.0)				
12	10.7 (0.0)				
13	16.8 (0.0)				

^a Energies for **1a–1e** are relative to **1a**; for **10–13**, relative to **11a**; for conformational shapes **a–e**, refer to **1a–1e** (Figure 2). ^b Parenthetical values correspond to percent populations obtained from a Boltzmann distribution at 25 °C. ^c Alternate protonated form **11a'**; see Table II and Scheme III.

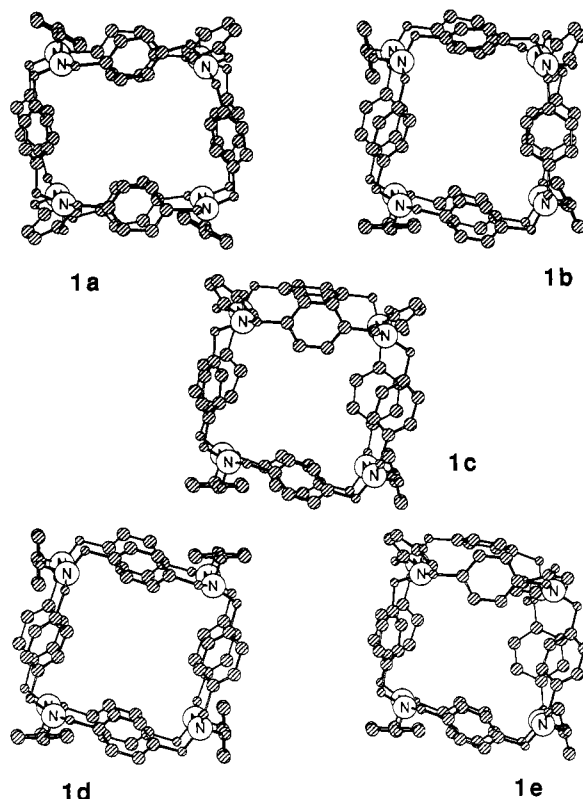
second-derivative Newton–Raphson optimization to convergence in Batchmin (30–60 min/structure). This third optimization step produced the **C_{2v}** conformation **1d**, 3.6 kcal above the ultimate low-energy minimum. No lower energy conformers could be located with this protocol even though the stochastic searching was allowed to continue for 60 cpu h. Attempts to introduce realistic aromatic π – π interactions into the no-hydrogen force field proved unsatisfactory. It was therefore abandoned, and the full all-hydrogen MM2 force field with the π features described above was employed.

Structure **1d** was used as a seed for the full treatment. In order to reduce searching times, a directed local strategy was adopted. In particular, only two edges on the Kyuphane idealized cube (**a**) were subjected to stochastic distortion as depicted in Scheme I. N to N corner atoms including a total of 18 atoms is regarded as an edge. The whole molecule, however, was refined through the two levels of Newton–Raphson optimization.

A new conformer (**1b**), 1.5 kcal lower than **1d**, was located after 24 cpu h of VAX 8650 searching. With **1b** as the starting structure, searches were conducted with the edge pairs indicated in (b) and (c) (Scheme I). Search (b) for 96 cpu h led to structures **1c** and **1e** (0.4 and 3.3 kcal higher than **1b**, respectively). Combination (c) was conducted for 186 cpu h, yielding multiple forms of **1b**, **1c**, and **1e**. In addition, a new low-energy conformer (**1a**), 2.1 kcal lower in energy than **1b**, was found four times. A number of additional Monte Carlo searches using **1a** as the starting structure were unproductive in locating any new conformations lower than the manifold represented by **1a–1e** (Table I, Figure 2). It must be emphasized, however, that the searches were not run to completion according to BAKMDL's stopping criterion: 50 duplicates of the lowest energy structure within 1-kcal energy window.

Two further searches were conducted to investigate the question of nitrogen lone pair inversion. Structure **1b** was modified by means of interactive SYBYL²⁵ graphics to produce partly refined invertomers with one (N7-in) and two (N6-in) N lone pairs directed outside the Kyuphane cage. The former delivered **1e** as the lowest energy N7-in species and relocated copies of **1b–1d** following the combined MODEL/MacroModel treatment. The latter N6-in, after 1.5–4.5 days of searching, provided no fully optimized structure lower than 16 kcal above conformation **1a**.

Charged Conformations. DelPhi Solvation. For each of the neutral conformations **1a–1e**, four of the N lone pairs were replaced by N⁺–H according to the first two protonation themes in Scheme II (● = NH⁺)

**Figure 2.** Five lowest energy Kyuphane conformations (**1a–1e**) as obtained by Monte Carlo searching and MM2 optimization (see text).**Table II.** Electrostatic Component of the Aqueous Solvation Energy for Kyuphane Tetracation **10** and **11** Conformations (298 K, kcal/mol)^{a,b}

protonation scheme ^c	$\Delta G_{\text{electrostatic}}^d$		E_{sol}^e	$\Delta E_{\text{sol}}(\text{rel})$	$\Delta \Delta E_{\text{sol}}^f$ (tet – sp)
	vacuum ($D = 1.0$)	solvent ($D = 80.0$)			
10a	736.6	380.7	–355.9	10.4	
11a	762.3	396.0	–366.3	0.0	10.4 (15.3)
11a'	716.0	349.4	–366.6	–0.3	10.7 (11.7)
10b	730.8	376.8	–354.0	12.3	
11b	756.6	393.9	–362.7	3.6	8.7 (17.8)
10c	710.6	356.2	–354.4	11.9	
11c	755.2	393.8	–361.4	4.9	7.0 (17.1)
10d	736.2	381.5	–354.7	11.6	
11d	723.8	361.1	–362.7	3.6	8.0 (14.0)
10e	732.3	373.9	–358.4	7.9	
11e	681.6	317.2	–364.4	1.9	6.0 (13.3)

^a Poisson–Boltzmann equation; cf. refs 26 and 27. ^b PRDDO charges. ^c Structure **10**, tetrahedral; **11**, square planar in NH⁺ arrangement; cf. Schemes II and III; for conformational shapes **a–e**, refer to **1a–1e** (Figure 2). ^d In units of RT; D = dielectric constant. ^e $E_{\text{sol}} = [\Delta G_{\text{solvent}}(D = 80.0) - \Delta G_{\text{vacuum}}(D = 1.0)]/0.5921$ (see text); the Gasteiger–Marsili values range from –368 to –386 kcal/mol. ^f Gasteiger–Marsili charges result in parentheses. Key: tet, tetrahedral; sp, square planar in NH⁺ arrangement.

to give tetracation isomers **10** and **11**. In addition, the low-energy conformer **1a** was protonated to give cations **12** and **13** (Scheme II).

The tetracations were then subjected to MM2 optimization in Batchmin. Relative energies are given in Table I. A rudimentary assessment of relative solvation energies is provided by an electrostatic potential calculation employing a finite difference solution to the Poisson–Boltzmann equation (DelPhi).^{26–28} The electrostatic component for each tetracation was evaluated at a dielectric constant of 2.0 for the molecule and 1.0 and 80.0 for the surrounding media. For the latter, the physiological ionic strength of 0.145 M has been used. The value pro-

(26) Gilson, M.; Sharp, K.; Honig, B. *J. Comput. Chem.* **1988**, *9*, 327–335.(27) Gilson, M.; Honig, B. *Proteins* **1988**, *4*, 7–18.

(28) Biosym Technologies, 10065 Barnes Canyon Road, San Diego, CA 92121; cf. DelPhi Release Notes 2.1, Section 2.6, June, 1990.

(25) Available from Tripos Associates, 1699 South Hanley Road, Suite 303, St. Louis, MO 63144.

Table III. Relative MM2 Approximate Solution Energies [$\Delta E_{\text{MM2}}(\text{rel})^a + \Delta E_{\text{sol}}(\text{rel})^b$] for Kyuphane Tetracation Conformations (kcal/mol)

	conformation				
	a	b	c	d	e
10	10.9	12.7	13.4	14.7	11.6
11	0.0	12.1	12.6	10.5	12.2
	10.5 ^c				

^a Table I. ^b Table II. ^c Alternate protonated from **11a'**; see Table II and Scheme III.

vides a reasonable estimate for the free energy of hydration of the trimethylammonium cation (see below). Since small variations in ionic strength have a negligible effect on calculated hydration energies,²⁷ the well-separated solvent shells of the individual, trisubstituted cationic NH^+ centers in **10** and **11** are expected to be suitably modeled in this way. Each of the conformations was maintained in a constant grid with the following characteristics defined initially by a calculation for **10a**: 65 points per side, total extent 25.804 Å, 0.403 Å/grid point, border space 5.0 Å. Gasteiger–Marsili charges^{29,30} as provided by SYBYL were employed in one set of calculations, PRDDO^{31,32} approximate ab initio Mulliken charges, in another. The difference [$\Delta G_{\text{solvent}}(D = 80.0) - \Delta G_{\text{vacuum}}(D = 1.0)$] then yields an estimate of the electrostatic contribution to the aqueous solvation energy.^{27,28} The relative values $\Delta E_{\text{sol}}(\text{rel})$ are given in Table II, while approximate relative solution energies are recorded as [$\Delta E_{\text{MM2}}(\text{rel}) + \Delta E_{\text{sol}}(\text{rel})$] in Table III. Similarly, three simple ammonium cations (NH_4^+ , CH_3NH_3^+ , $(\text{CH}_3)_3\text{NH}^+$) were optimized by MacroModel, supplemented with PRDDO charges, and subjected to a DelPhi calculation (65 points per side, border space 5.0 Å, 0.215 Å/grid point). As an example, the calculation for CH_3NH_3^+ gave $\Delta G_{\text{solvent}}(D = 80.0) = 481.0$ and $\Delta G_{\text{vacuum}}(D = 1.0) = 624.2$ in units of RT . These are converted to kilocalories per mole at 298 K with the factor 0.5921 ($=0.001987 \times 298$). Then $E_{\text{sol}} = 284.8 - 369.6 = -84.8$ kcal/mol. The resulting free energies of hydration for the three ammonium cations are -100.5, -84.8, and -64.9 kcal/mol, respectively. The corresponding experimental ΔG_{sol} values are NH_4^+ , -78,³³ -79;³⁴ CH_3NH_3^+ , -68,³³ -70;³⁵ and $(\text{CH}_3)_3\text{NH}^+$, -59,³⁴ -61 kcal/mol.³³

Current quantum mechanical programs generally cannot treat a molecule as large as Kyuphane (**1**) or its cations. PRDDO is no exception. Atomic charges were therefore calculated for $\text{HN}^+(\text{CH}_2\text{-Ph-CH}_2\text{-NH}_2\text{X})_3$ and $\text{:N}(\text{CH}_2\text{-Ph-CH}_2\text{-NH}_2\text{X})_3$ ($\text{X} = \text{H}^+$ or lone pair) with one, two, and three formal charges on the Kyuphane substructures. Molecular geometries were taken from the MM2-optimized structure of **10a**. The resulting charge distribution was placed at the appropriate C, N, and H atoms for **10** and **11** and balanced to give a total molecular charge of +4.

Molecular Volumes. Kyuphane Cavity Size. An attempt to estimate the cavity volume for the various Kyuphane conformations was made by using Connolly's adaptation^{36,37} of the Richards' procedure.^{38,39} The method calculates a molecular surface area by rolling a spherical probe across the structure of interest represented as an envelope of a set of interpenetrating spheres. MM2 van der Waals values were used here. In a second step, the volume of the molecule enclosed by the surface is calculated.

To obtain the approximate size of the Kyuphane complexation site, a small probe ($r = 1.0$ – 1.4 Å) capable of entering the cavity was first employed. This yields the volume encased by both inner and outer surfaces. Secondly, a larger probe ($r = 3.0$ – 4.5 Å) capable only of creating a molecular surface around the exterior of the particle was used. A reentrant surface^{36–39} across the holes in each Kyuphane cubical face is necessarily produced. The volume of this second total molecular surface includes the interior cavity. The difference between the volumes

Table IV. Molecular Volumes^a for Neutral and Tetracation Kyuphane Conformations: Estimate of Kyuphane Cavity Size ΔV (Å³)

	probe size, r (Å)				ΔV_1^b	ΔV_2^b	ΔV^c
	1.0	1.4	3.0	4.5			
1a	1835	1911	2151	2221	240	386	313
1b	1819	1896	2167	2242	271	423	347
1c	1826	1910	2172	2245	262	419	341
1d	1805	1867	2175	2259	308	454	381
1e	1842	1916	2153	2220	237	378	308
10a	1862	1925	2179	2246	254	384	319
10b	1844	1932	2184	2250	252	406	329
10c	1846	1944	2190	2254	246	408	327
10d	1821	1926	2194	2267	268	446	357
10e	1858	1947	2175	2237	228	379	304

^a By the procedure of refs 36 and 37. ^b The smallest (ΔV_1) and largest (ΔV_2) volume differences between probes 1.0/1.4 and 3.0/4.5 Å. ^c The average of the four differences between 1.0/1.4- and 3.0/4.5-Å probe calculations.

Table V. Molecular Volumes^a for Various Kyuphane Guests (Å³)

guest	probe size, r (Å)				\bar{V}^b
	1.0	1.4	3.0	4.5	
benzene	116	117	120	121	119
chloroform	104	105	107	109	106
naphthalene	172	173	177	180	176
pyrene	246	248	253	256	251
perylene	300	302	309	314	306
ANS	329	334	349	361	343
TNS	332	337	353	366	347
α -PNA	282	286	296	305	292
β -PNA	281	285	296	303	291
1-DAN	239	242	251	259	248
1-NS	220	222	228	232	226
2-NS	221	222	230	233	227
2,7-NDS	270	273	282	287	278
2,6-NDS	270	273	282	287	278
1,5-NDS	266	270	279	285	275
10-CS	276	280	291	297	286

^a By the procedure of refs 36 and 37. ^b Volume average for the four probes.

provided by the small and the large probes yields an estimate of the "free" volume inside the host for a given conformation. The results for various probe sizes are tabulated for Kyuphane conformations in Table IV. The Connolly molecular volumes of various guests are likewise recorded in Table V.

Kyuphane Complexes. Several small molecules were merged into the central cavity of conformation **10a** by means of the SYBYL software. In each case, the complexes were passed into MacroModel for addition of N or O lone pairs and then optimized to convergence with MM2/Batchmin. In some cases, the guest was repositioned in a different starting orientation in the host cavity and reoptimized.

Results and Discussion

Among various macrocyclic hosts with a cyclophane unit previously reported, those constructed with a 2,11,20,29-tetraaza[3.3.3.3]paracyclophane ring as a basic macrocyclic skeleton have been widely examined in various media. N,N',N'',N''' -Tetramethyl-2,11,20,29-tetraaza[3.3.3.3]paracyclophane (**9**), first prepared by Yoshino et al.,⁴⁰ tends to form stable inclusion complexes with small organic molecules, such as benzene, dioxane, chloroform, dichloromethane, bromochloromethane, and acetonitrile, in the crystalline state.^{40–42} Accordingly, a hydrophobic cavity provided by the [3.3.3.3]paracyclophane ring would seem to be relatively small for incorporation of larger hydrophobic guests

(29) Gasteiger, J.; Marsili, M. *Tetrahedron* **1980**, *36*, 3219–3228.

(30) Marsili, M.; Gasteiger, J. *Croat. Chem. Acta* **1980**, *53*, 601–614.

(31) Halgren, T. A.; Lipscomb, W. N. *J. Chem. Phys.* **1973**, *58*, 1569–1591.

(32) Marynick, D. S.; Lipscomb, W. N. *Proc. Natl. Acad. Sci. U.S.A.* **1982**, *79*, 1341–1345.

(33) Aue, D. H.; Webb, H. M.; Bowers, M. T. *J. Am. Chem. Soc.* **1976**, *98*, 318–329.

(34) Pearson, R. G. *J. Am. Chem. Soc.* **1986**, *108*, 6109–6114.

(35) Cabani, S.; Gianni, P.; Mollica, V.; Lepori, L. *J. Solution Chem.* **1981**, *10*, 563–595.

(36) Connolly, M. L. *J. Appl. Crystallogr.* **1983**, *221*, 548–558.

(37) Connolly, M. L. *J. Appl. Crystallogr.* **1983**, *221*, 709–713.

(38) Richards, F. M. *Annu. Rev. Biophys. Bioeng.* **1978**, *6*, 151–176.

(39) Richmond, T. J.; Richards, F. M. *J. Med. Biol.* **1978**, *119*, 537–555.

(40) Urushigawa, Y.; Inazu, T.; Yoshino, T. *Bull. Chem. Soc. Jpn.* **1971**, *44*, 2546–2547.

(41) Abbott, S. J.; Barrett, A. G. M.; Godfrey, C. R. A.; Kaljindjian, S. J.; Simpson, G. W.; Williams, D. J. *J. Chem. Soc., Chem. Commun.* **1982**, 796–797.

(42) Tabushi, I.; Yamamura, K.; Nonoguchi, H.; Hirotsu, K.; Higuchi, T. *J. Am. Chem. Soc.* **1984**, *106*, 2621–2625.

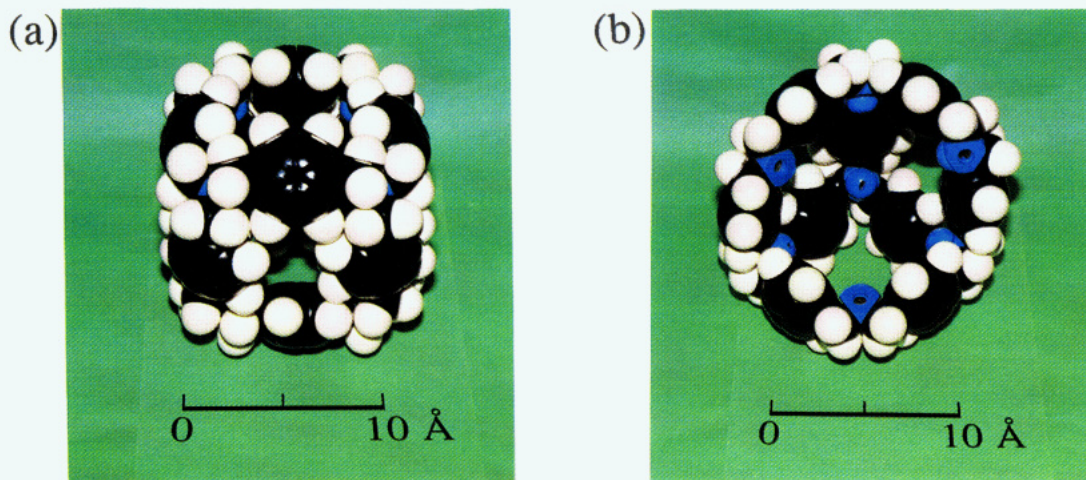


Figure 3. CPK molecular model of Kyuphane (**1**): (a) complete view; (b) three *p*-xylylene moieties are removed to show the amino nitrogens (blue color) whose lone pair orbitals are directed toward the interior cavity.

such as ANS. Indeed, the binding constant (K) for the 1:1 host-guest complex with ANS in aqueous media is only moderate: $K = 380 \text{ M}^{-1}$ at pH 4.2.⁴³ A microenvironment around the complexation site as evaluated from the fluorescence maximum of ANS is polar and close to that in water.^{43,44} In order to improve the molecular recognition ability of the azacyclophane host toward hydrophobic guest molecules, it became necessary to construct a larger and more hydrophobic three-dimensional cavity by appropriate chemical modifications of the single macrocyclic skeleton. For these reasons, we designed and prepared a new cage-type host, Kyuphane (**1**). The molecule provides a relatively rigid and large hydrophobic cavity surrounded by six faces, each being constructed with the 2,11,20,29-tetraaza[3.3.3.3]paracyclophane ring. In order to better evaluate the molecular recognition ability of the hydrophobic molecular cage provided by Kyuphane, we also prepared the corresponding noncage host (**2**), in which four covalent bonds forming one of the macrocyclic rings of Kyuphane are disconnected; this modification turns out to give a 2,11,20,29-tetraaza[3.3.3.3]paracyclophane derivative with four hydrophobic and bulky branches.

Structural Characteristics of Kyuphane. NMR and Conformation. Examination of a CPK molecular model of **1** reveals a globular hydrophobic cavity with a maximum inner diameter of ca. 9 Å for the van der Waals surface. Only guest molecules capable of passing through the tetraaza[3.3.3.3]paracyclophane ring (hole size 5.5–7 Å) can be incorporated into the inner cavity (Figure 3).

Comparative rigidity in the molecular framework of Kyuphane is reflected by its ^1H NMR (400 MHz) signals. In $\text{DCON}(\text{CD}_3)_2$ at 298 K, both phenyl and methylene proton signals appear as broad singlets at $\delta = 7.28$ and 3.40 ppm with half-bandwidths ($\Delta\nu_{1/2}$) of 160 and 176 Hz, respectively (Figure 4b). These signals are little changed in their broadness even at high temperatures; $\Delta\nu_{1/2}$ values are 144 and 128 Hz for the phenyl and methylene signals at 398 K, respectively (Figure 4a). In $\text{CDCl}_3\text{-CS}_2$ (3:7 v/v) at 298 K, $\Delta\nu_{1/2}$ values are 156 and 172 Hz for the phenyl and methylene signals, respectively, and nearly identical with those measured in $\text{DCON}(\text{CD}_3)_2$ at the same temperature. When the measurement temperature was lowered in $\text{CDCl}_3\text{-CS}_2$ (3:7 v/v), broadening of these signals was gradually enhanced (Figure 4c and d) until each of the signals was split into a broad doublet (Figure 4e and f). The apparent coalescence temperatures (T_c) evaluated for the phenyl and methylene signals are different. T_c values are ca. 200 and ca. 220 K for the phenyl and methylene proton signals, respectively. This suggests that molecular motion of the methylene moieties is more restricted than that of the phenyl

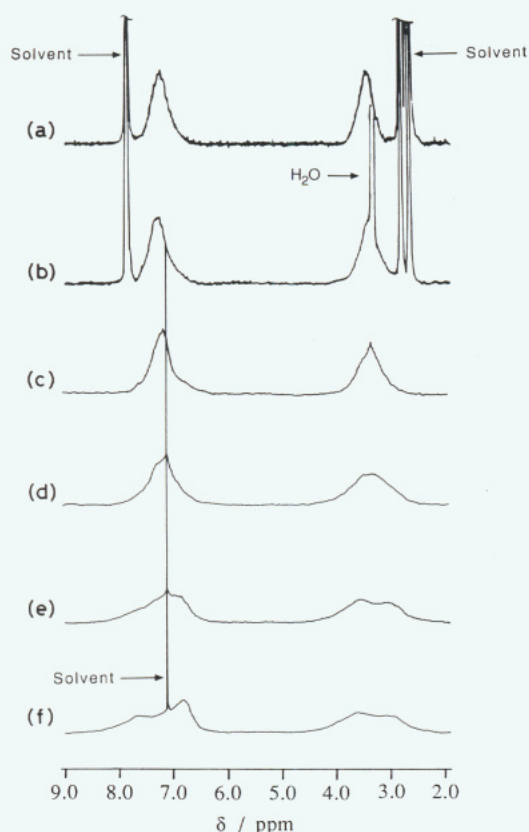


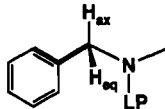
Figure 4. ^1H NMR spectra of Kyuphane at (a) 398, (b) 298, (c) 273, (d) 223, (e) 198, and (f) 173 K in the following solvents: $\text{DCON}(\text{CD}_3)_2$, (a) and (b); $\text{CDCl}_3\text{-CS}_2$ (3:7 v/v), (c)–(f).

rings as indicated by the CPK model. As for the corresponding simple macrocycle (**9**) in the identical solvent, the T_c value for the phenyl proton signal is 183 K. Coalescence for the methylene proton signal was not observed in the 293–173 K temperature range. In addition, the significant signal broadening observed for Kyuphane was not seen for **9** and the noncage host **2** in organic solvents. Thus by comparison, the intramolecular rotational freedom of the molecular components of Kyuphane is highly suppressed in solution as a result of the semirigid structural features of the cubic framework.

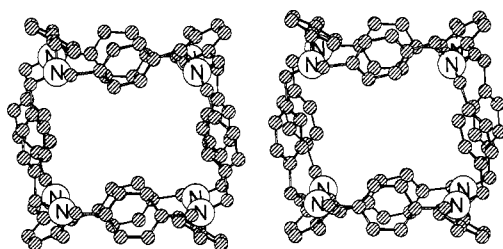
Low-energy conformations of Kyuphane (**1**) were examined by a stochastic search in excess of 2 cpu weeks on a VAX 8650 coupled to molecular mechanics (MM2) refinement. Five low-energy conformations within 5.5 kcal were obtained. Since the search was not run to completion (see Computational Methods), we have no guarantee that the global minimum has been located.

(43) Tabushi, I.; Kuroda, Y.; Kimura, Y. *Tetrahedron Lett.* **1976**, 3327–3330.

(44) Tabushi, I.; Kimura, Y.; Yamamura, K. *J. Am. Chem. Soc.* **1981**, *103*, 6486–6492.

Table VI. Torsional Angles Φ at the Corner of Kyuphane Conformer **1a** as a Function of Diagonal Distance


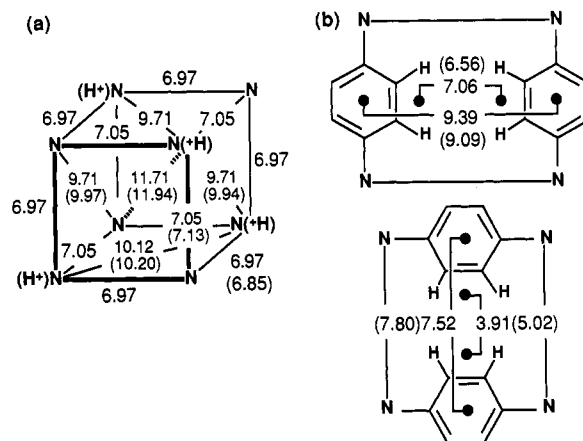
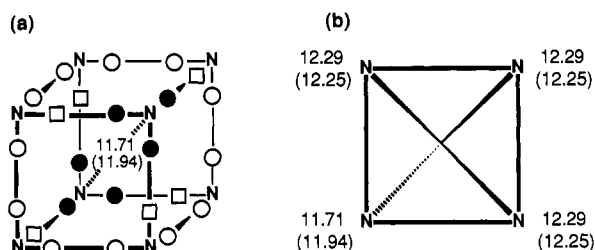
diagonal distance ^a (Å)	$\Phi(\text{CC-CH}_{\text{ax}})$ (deg)	$\Phi(\text{CC-CH}_{\text{eq}})$ (deg)	$\Phi(\text{H}_{\text{ax}}\text{C-NLP})$ (deg)	$\Phi(\text{H}_{\text{eq}}\text{C-NLP})$ (deg)
11.7	25.3	-81.1	-74.1	168.0
12.3	-0.9	-107.1	-73.6	169.0
12.3	-6.2	-111.5	-80.4	162.4
12.3	-7.3	-113.0	-73.6	169.0

^a Refer to Figure 7 for a schematic of the different corner positions.**Figure 5.** Lowest energy MM2-optimized Kyuphane conformation of C_i symmetry (**1a**), stereo view.

However, the Monte Carlo search procedure employed²¹ favors the low-energy regions of conformation space. This is especially true when low-energy structures are used as seeds in subsequent searches, a strategy adopted repeatedly for the minimum energy conformations of **1**. In any case, the richness of the conformational profile provides an opportunity to better understand both the temperature-dependent NMR spectra and the guest-selective complexation properties. The five minima are pictured in Figure 2. The lowest (**1a**) belongs to the C_i symmetry point group with a center of inversion or equivalently a 2-fold axis of improper rotation (S_2) as the relevant symmetry element. The optimized structure is pictured in stereo in Figure 5. Conformer **1a** corresponds to 91.6% of the calculated equilibrium mixture by a Boltzmann distribution at 25 °C (Table I). Conformer **1d** is the only other member of the set with symmetry (C_{2v}), the remainder (**1b**, **1c**, **1e**) belonging to the trivial C_1 point group.

Various interatomic distances found for conformation **1a** are depicted in Figure 6. The C_i symmetry of the structure is nicely illustrated by the existence of three corner-to-corner diagonals of 12.3 Å and a fourth of 11.7 Å (Figure 7). The CH_2 groups of **1a** are diastereotopic, one proton approximately trans to the nitrogen lone electron pair, the other gauche. An analysis of the corner torsional angles reveals that the CH_2 's reside in three different environments relative to the adjacent benzene rings. This places them in somewhat different regions of the aromatic NMR shielding cone. Table VI lists the angles and Figure 7a provides a schematic of their location. The figure demonstrates that all atoms come in symmetry-related pairs, a consequence of the overall C_i symmetry. All three CH_2 's at the ends of the 11.7-Å diagonal are equivalent, while the CH_2 's at the corners of the longer 12.3-Å diagonal are split between two environments. The structure as a dynamic entity can populate at least eight degenerate C_i conformations. Thus, the short diagonal can be found spanning four separate pairs of corners. For each of these, the diastereotopic CH_2 's can exist in either the trans/gauche or gauche/trans orientation relative to the N lone pair. In addition, there are less pronounced local fluctuations that seem possible as a result of the small but real $\Phi(\text{HC-NLP})$ differences for the CH_2 's at the ends of the long diagonals (Table VI). Finally, the phenyl rings are likewise free to rotate.

Below -50 °C in $\text{CDCl}_3\text{-CS}_2$, the methylene protons of **1** split into a broad ill-defined doublet in the NMR. In light of the conformational analysis, this observation can be interpreted as follows. If conformer **1a** were the dominant Kyuphane species in solution, all eight degenerate cage forms, the twelve phenyl

**Figure 6.** Various intracage distances (Å) for MM2-optimized conformations **1a** and **10a**. In (b), the separations are between centers of the phenyl rings and the ortho hydrogens, respectively. Parenthetical values belong to **10a**.**Figure 7.** C_i symmetry of **1a** and **10a** as illustrated by (a) three different environments for the CH_2 's bonded to N and (b) the $\text{N}\cdots\text{N}$ diagonal distances (Å). Parenthetical values belong to **10a**.

rotations, and any local movements would need to be rapidly scrambled to observe sharp peaks in the NMR. As the pathway between the degenerate forms is likely to be complex and to involve passage through several intermediate stages, the broad signals are unresolved at all temperatures. Alternatively, the MM2 energy spread of 5.4 kcal for **1** reported in Table I may be larger than in the actual experimental situation, or the stochastic search may have missed other conformers within 1–2 kcal of **1a**. In these cases, the broad-band NMR's of Figure 4 imply slow interconversion among a set of distinct isoenergetic conformations superimposed on exchange among the degenerate species of each of them. We cannot firmly distinguish between the two explanations at this time.

An additional feature of Kyuphane's conformational manifold concerns the inversion state of the eight nitrogen lone electron pairs. Isomers **1a–1d** are N8-in forms, all eight lone pairs pointing into the central cavity. The fifth and highest energy conformer **1e** is a N7-in species with a N lone pair directed outward into the solvent medium. This N7-in structure was located both from **1b** and from an arbitrarily crafted N7-in variant employed as a search seed. The strain energy evident in **1e** is amplified in the N6-in species. No energetically competitive examples of the latter

were found from an independent Monte Carlo search employing a N6-in variant as a starting structure.

The prediction that energetically viable conformers of Kyuphane (**1**) are of the N8-in variety is satisfying. It accords with the intuitive expectation that lone pair accepting guests are best served by the opportunity to explore a maximum of binding interactions.

Kyuphane Cavity and Face Dimensions. Distances within the cavity of Kyuphane **1a** as given in Figures 5 and 6 are reflective of guest occupation when diminished by the van der Waals radii of nitrogen. Taking this as the MM2 value of 1.7 Å, the opposite surfaces of the internal cavity are separated by a maximum of 8.3–8.9 Å. A fully encompassed guest's largest dimension must fall within these boundaries.

Another measure of guest size is the maximum free volume circumscribed by Kyuphane's inner van der Waals surface. Since six of the molecule's faces are open to solvent and different conformations are available to the system, a precise definition is not possible. A reasonable estimate is given by the simple average value \bar{V} for a given conformation, which ranges from 308 to 381 Å³ for **1a–1e** (Table IV). A Boltzmann weighted average applicable to the latter equilibrium (298 K) is calculated to be 315 Å³ from the energies of Table I and the \bar{V} 's of Table IV. A complementary measure of Kyuphane cavity volume can be obtained as follows. Conformation **10a** of the tetrahedral tetracation was solvated inside and out with explicit water molecules⁴⁵ by means of the AMBER protocol.⁴⁶ Eight water molecules are found within the cavity, four of which are located approximately at the center of four corner nitrogens defining four different Kyuphane faces. Extraction of these water molecules followed by calculation of their combined volume with probes of different size leads to an average volume $\bar{V} = 307$ Å³.

With allowance made for slight Kyuphane host expansion, a completely encapsulated guest with its longest dimension (8.8–9.0 Å) can possess a van der Waals volume of not much more than 300 Å³. The same restriction applies to both nonionic and cationic conformations. Strongly bound guests with larger molecular volumes must necessarily expose part of their structure to solvent, presumably by extending outward through at least one of the Kyuphane faces.

Entrance into the host's cavity requires penetration of one of the molecule's faces. As recorded in Figure 6b, the smallest phenyl–phenyl and edge–edge distances for **1a** are 7.5 and 3.9 Å, respectively. Reduced by van der Waals radii (MM2: C, 1.85; H, 1.50 Å) the separations become 3.7 and 0.9 Å. The apparent open architecture of the line drawings in Figures 2 and 5 gives way to a bottleneck of seemingly small proportion. The finding of single AMBER water molecules in the cage faces reinforces this view. Encapsulation of a guest by **1** is a dynamic process and obviously requires considerable phenyl rotation and molecular breathing.

Molecular Recognition by Kyuphane as a Nonionic Host. The simple macrocyclic host **9** undergoes complexation with various solvent molecules in the solid state at the 1:1 molar ratio of host to guest.^{40–42} Since each face of Kyuphane is constructed with a macrocyclic ring identical with that of **9**, host–guest complexes are expected to be formed from Kyuphane and various organic molecules. In fact, when Kyuphane was solidified from its benzene solution, we obtained a Kyuphane–benzene (1:1) complex. Kyuphane also includes chloroform in a 1:1 molar ratio. Tabushi et al. reported that the host–guest inclusion complex of **9** with chloroform in the crystalline state was decomposed with the concomitant total loss of the guest upon heating at 80 °C (0.5 mmHg) for 4 h.⁴² By contrast, the C–Cl stretching mode intensity for the Kyuphane–chloroform complex remained unchanged even after heating at 100 °C (0.1 mmHg) for 4 h. The IR intensity gradually decreased at 100 °C (0.05 mmHg), and the band disappeared completely after 18 h of heating. Thus, it seems that

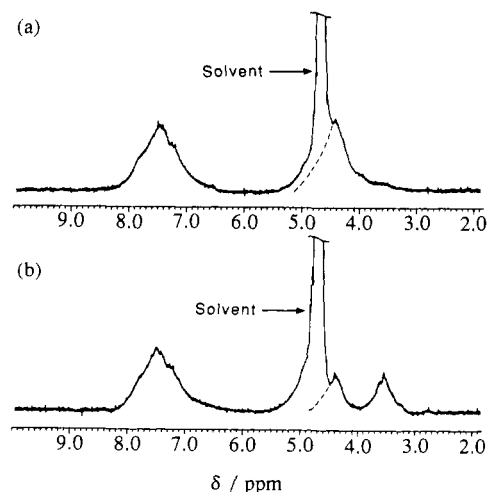


Figure 8. ¹H NMR spectra of Kyuphane in D₂O at 30.0 °C with [1,2-d₄]trimethylsilylpropionate (TSP) as an external reference: (a) pD 2.4, [1] = 1.5 mM; (b) pD 4.0, [1] = 120 μM.

Kyuphane incorporates organic guest molecules into its hydrophobic cavity much more strongly than **9** in a 1:1 molar ratio in the solid state. Unfortunately, we were not able to obtain single crystals of the host and the host–guest complexes for X-ray crystallographic analysis. On the other hand, formation of the inclusion complex of Kyuphane with two chloroform molecules in solution was confirmed on the basis of a molecular weight measurement by osmometry.

The calculated Kyuphane cavity dimensions are in complete accord with the observation of tight complexes for benzene and chloroform. The molecular volumes \bar{V} of both solvents are well below 300 Å³ (Table V) as required for enclosed 1:1 complexes. Similarly, a pair of near-spherical chloroform molecules fills only a 212-Å³ volume, easily accommodated by the host's central cavity.

Protonation Geometries and Hydration Energies of a Tetracationic Host. Kyuphane is soluble in acidic aqueous media below pH 4. Dynamic light scattering (dls) measurements revealed that Kyuphane does not undergo aggregation under the medium conditions employed in this study, and that the critical aggregate concentration is larger than 2.0 mM if there is any aggregation tendency. Broad ¹H NMR signals were also observed for Kyuphane in cationic molecular forms in aqueous media. In a pD region below 2.5, broad singlet signals were observed in D₂O at δ = 7.47 and 4.39 ppm for the phenyl and methylene protons, respectively, indicating that all the amino nitrogens were completely protonated (Figure 8a). On the other hand, the methylene proton signal was separated at pD 4.0 into two broad singlets with identical peak areas at δ = 3.53 and 4.39 ppm (Figure 8b). Four amino nitrogens among all the tertiary amino moieties in Kyuphane are evidently protonated on the average.

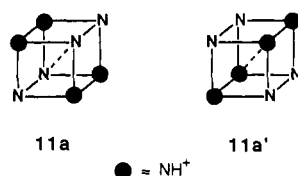
Examination of the conformational manifold for different protonation patterns of the tetracation illustrates a system of considerable complexity. The MM2 energies of Kyuphane tetracations are summarized in Table I. For the five conformations **a–e**, both tetrahedral and square-planar protonation patterns **10** and **11**, respectively, were evaluated. The S and face forms **12** and **13** were likewise optimized for C_i conformation **a** (Scheme II). The gas-phase force field energies posit conformer **a** to be the lowest energy species for both nonionic and protonated systems. A conformation without symmetry, **10b**, is within 0.4 kcal, while the C_{2v} conformation **10d** lies 3.1 kcal higher. In terms of a Boltzmann distribution of the MM2 optimized energies at 25 °C, the abundant conformations are **11a**, **10a**, **10b**, and **10c** with relative populations of 49, 21, 25, and 4%, respectively. By comparison with the nonionic Kyuphane, conformations **b** and **c** make a considerably enhanced gas-phase contribution.

The observation that tetravalent carbon adopts a tetrahedral rather than a square-planar arrangement is readily understood as a result of minimizing electron repulsion in the tetrahedral

(45) Rao, S. N. (Searle), private communication.

(46) Singh, U. C.; Weiner, P. K.; Cadwell, J. W.; Kollman, P. A., AMBER(UCSF) version 3.0 (1986), Department of Pharmaceutical Chemistry, University of California, San Francisco, CA 94143.

Scheme III



geometry. The same principle applies to the spatial distribution of four positive charges such as NH^+ . Why then does the "square-planar" form of tetraprotonated Kyuphane **11a** fall 0.5 kcal lower in energy (Table I) than the tetrahedral variant **10a**? Distance analysis of the two optimized conformations suggests a basis for the near energetic balance. Structure **10a** involves six distances between nitrogens of the NH^+ centers, three each at 9.94 and 10.20 Å (Figure 6). Protomer **11a** displays a window of NH^+ separations both shorter and longer than the latter: 6.98 (2 \times), 10.07 (2 \times), 12.15, and 12.35 Å. The simple average of the two sets is 10.1 and 9.8 Å for **10a** and **11a**, respectively. Though this raw comparison would suggest **11a** to be slightly less favorable, the remaining charge-charge interactions spread across the *p*-xylene bridges obviously compensate. The fact that the low-energy Kyuphane conformer **a** is only of C_i symmetry with one short diagonal (Figures 6 and 7) and several benzyl torsions (Table VI) provides the opportunity for a multitude of small but influential electrostatic interactions. Straightforward analysis based on only four atomic centers is thereby precluded.

A subtlety in the constitution of the minimum energy tetracation **11a** owes its origin to the existence of a single short C_i diagonal as pictured in Figure 7. When the NH^+ centers are located at the ends of the long diagonals, the lowest energy structure **11a** results. However, if the square-planar arrangement places two NH^+ centers at the termini of the short diagonal, geometry optimization yields a cationic variant 10.8 kcal higher, **11a'** (Scheme III). The evaluated gas-phase MM2 energy arises in part from the 0.5 Å closer approach of the two diagonally related NH^+ s. In addition, there exist two different face diagonal distances of 9.7 and 10.2 Å in the C_i structure (Figure 6a). Pattern **11a** incorporates the two long $\text{NH}^+\cdots\text{NH}^+$ values, whereas **11a'** brings both pairs of charged centers 0.4 Å closer. Other higher energy cation conformations **b-e** (Table I) experience a similar proton placement phenomenon. However, these have not been investigated.

The Kyuphane tetraammonium salt is described below in terms of its ability to bind a variety of small guest molecules. The complexing medium in each case is a buffered aqueous medium at pH's from 1.4 to 4.0. In an attempt to assess possible equilibrium components for the tetracation, we have employed Honig and colleagues' treatment of the Poisson-Boltzmann equation (DelPhi)²⁶⁻²⁸ as an estimate of aqueous solvation free energies. The method provides an electrostatic contribution to the latter, E_{sol} (Table II), modeled by the interaction of a molecule's atomic charges with an induced reaction field. Salt effects are accommodated by employing a term for ionic strength, taken to be 0.15 in the present case. As a test for the semiquantitative quality of the method, three simple ammonium cations (NH_4^+ , CH_3NH_3^+ , and $(\text{CH}_3)_3\text{NH}^+$) were subjected to the DelPhi procedure, and the results compared with measured hydration free energies (see Computational Methods). The method with its present parameters overestimates ΔG_{sol} by 23, 16, and 5 kcal/mol, respectively. However, the values are correctly ordered, and within 10–25% of experimental when PRDDO atomic charges are used.

Application of DelPhi to the tetracations **10** and **11** (**a-e**) using PRDDO and Gasteiger-Marsili charge schemes provides free energies of hydration within a -355- to -385-kcal/mol window (Table II). Each of the four charged centers on the average is thus estimated to be solvated by -89 to -96 kcal/mol. This is to be compared with the DelPhi $E_{\text{sol}} = -64.9$ and -84.9 kcal/mol for $(\text{CH}_3)_3\text{NH}^+$ and CH_3NH_3^+ , respectively. The apparent estimated hydration energy increase per cationic head can be understood as both short- and long-range charge dispersal along the

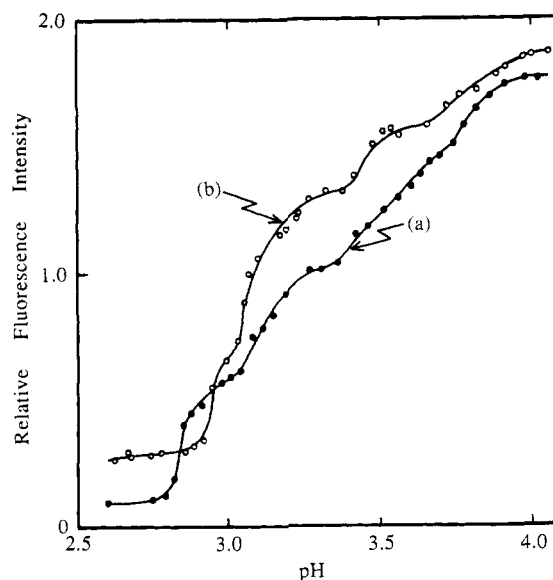


Figure 9. Correlations of fluorescence intensities of ANS (a) and TNS (b) (1.0 μM each) with pH upon addition of Kyuphane (10 μM) in aqueous acetate buffer (10 mM, μ 0.10 with KCl) at 30.0 °C. Excitation and emission wavelengths are 375 and 462 nm for ANS and 324 and 428 nm for TNS, respectively.

12 *p*-xylyl ribbons connecting the cage corners.

An additional aspect of the DelPhi treatment is the suggestion that the square-planar protonation topology (i.e., **11**) is 6–11 kcal/mol more stabilized by aqueous solvation than the tetrahedral proton placement (Table II). Summation of the optimized force field steric energy, $\Delta E_{\text{MM2}}(\text{rel})$, and the DelPhi solvation energy, $\Delta E_{\text{sol}}(\text{rel})$, provides an approximate solution energy for the Kyuphane tetracations (Table III). Similar to the outcome for nonionic cage **1**, a single conformation is predicted to obtain in the aqueous milieu, i.e., the square-planar C_i species **11a**. Given the underlying approximations leading to this conclusion, the population result cannot be taken with certainty. Nevertheless, the doublet nature of the Kyuphane methylene protons in the NMR at pD 4.0 (Figure 8) is consistent with the C_i conformation represented by either a square-planar or a tetrahedrally protonated species. The acidified solution is most likely a mixture of **10a** and **11a**, with the latter predominating. Members of the equilibrium undoubtedly experience rapid proton exchange superimposed on conformational interchange similar to that described above for nonionic Kyuphane (**1**).

Microenvironmental Properties of the Kyuphane Cavity. Even though we repeatedly tried to evaluate pK_a values for Kyuphane by means of potentiometric titration, reliable values could not be obtained because of its low solubility in aqueous media at higher pH's. Therefore, we examined the pH-dependent microenvironmental properties of the internal cavity of Kyuphane as experienced by the anionic and hydrophobic fluorescent probes ANS and TNS. The fluorescence intensity increased along with a concomitant blue shift of the fluorescence maximum in the presence of Kyuphane as the medium pH was raised.^{15c} This behavior indicates that hydrophobicity in the internal cavity of Kyuphane is enhanced as the extent of protonation at the nitrogen atoms decreases. Four stepwise proton dissociation equilibria for the host-guest complexes composed of Kyuphane and the fluorescent probes were determined in the pH range of 2.5–4.0 by fluorescence spectroscopic titration (Figure 9): pK_1 , 2.85; pK_2 , 3.15; pK_3 , 3.5; pK_4 , 3.8 for ANS; pK_1 , 2.95; pK_2 , 3.1; pK_3 , 3.45; pK_4 , 3.8 for TNS.

On the other hand, each of the fluorescence maxima originating from ANS (λ_{max} 463 nm) and TNS (λ_{max} 430 nm) is independent of the medium pH in the presence of the noncage host **2**, while the fluorescence intensities increase as the medium pH is raised. We carried out fluorescence spectroscopic titration with the identical fluorescent probes. A single acid dissociation equilibrium with a pK_a value of 3.3 was found in the pH range of 2.5–4.0.

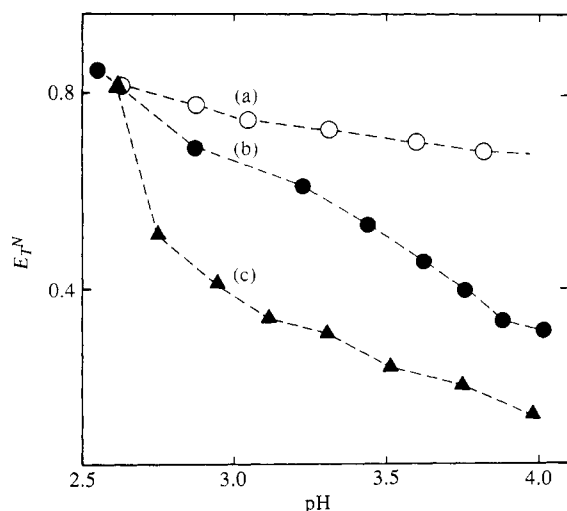


Figure 10. pH-dependent variations of microenvironmental polarity experienced by TNS (a), ANS (b), and α -PNA (c) in the internal cavity of Kyuphane, in aqueous acetate buffer (10 mM, μ 0.10 with KCl) at 30.0 °C.

Table VII. Binding Constants (K) for 1:1 Host–Guest Complexes of Azacyclophanes with Fluorescent Guests in Aqueous Acetate Buffer (10 mM, μ 0.10 with KCl) at 30.0 °C^a

host	pH	K (M ⁻¹)		
		ANS	TNS	α -PNA
1	2.6	3.8×10^3	4.6×10^3	
	3.0	1.0×10^4	3.0×10^4	8.9×10^2
	4.0	1.6×10^5	4.2×10^5	8.8×10^4
2	3.0		1.1×10^3	
	4.0	1.1×10^3	3.2×10^3	2.1×10^3

^a Concentrations: guests, 1.0×10^{-6} M; 1, 1.0×10^{-5} to 6.0×10^{-5} M; 2, 1.0×10^{-5} to 2.0×10^{-5} M.

Insufficient solubility of host **2** at higher pH's precluded determination of other pK_a values. Tabushi et al. have reported that pK_1 and pK_2 values for the simple tetraaza[3.3.3]paracyclophane **9** are 3.0 and ca. 6, respectively, by means of potentiometric titration,⁴³ the former value being comparable to that for **2** as evaluated here by fluorescence spectroscopy. Thus, it seems that there is little intramolecular interaction between the amino moieties in the macrocyclic ring and those in the side arms of **2** to influence the pK_a values. This is in marked contrast with our observation for Kyuphane, multiple pK_a values in the same pH region. Accordingly, the unique acid dissociation behavior of Kyuphane most likely arises from the N8-in configuration as suggested by the CPK model study and the MM2 calculations (vide supra).

The microenvironmental polarity parameter, E_T^N ,⁴⁷ was evaluated from the maximum emission wavelength due to a fluorescent probe incorporated into the host in a manner similar to that reported previously.^{7b} The pH-dependent E_T^N values for ANS, TNS, and α -PNA in the presence of Kyuphane are shown in Figure 10. The E_T^N value for anionic ANS, a guest with a molecular volume slightly greater than the 300-Å³ ideal (Table V), varied from 0.873 to 0.302 as the pH was raised from 2.5 to 4.0. This is to be compared with reference E_T^N values of 0.886 and 0.309 for 2,2,3,3-tetrafluoro-1-propanol and dichloromethane, respectively. The nonionic α -PNA with a molecular volume 85% that of ANS (Table V) experienced an even greater pH dependence of the micropolarity. However, the micropolarity experienced by the anionic TNS, a molecule slenderer than ANS and 2.5–3.0 Å longer than the van der Waals diameter of the inner cavity of Kyuphane, varied to a lesser extent as the medium pH was varied. Thus, the internal molecular cage of Kyuphane provides a specific microenvironment that undergoes drastic change as a result of protonating and deprotonating the amino moieties.

Table VIII. Binding Constants (K) for 1:1 Host–Guest Complexes of Kyuphane (**1**) with Nonionic Guests in Aqueous Acetate Buffer (10 mM, μ 0.10 with KCl, pH 4.0) at 30.0 °C^{a,b}

guest	K (M ⁻¹)
perylene	7.1×10^2
pyrene	5.6×10^3
α -PNA	8.8×10^4
β -PNA	6.9×10^4
1-(dimethylamino)naphthalene (1-DAN)	2.7×10^4
naphthalene	3.0×10^3
1,3-dihydroxynaphthalene (1,3-DHN)	c

^a Concentrations: guests, 1.0×10^{-7} to 1.0×10^{-6} M; **1**, 1.0×10^5 to 3.0×10^5 M. ^b Benesi–Hildebrand treatment of fluorescence data. ^c Complex formation was not detected.

Table IX. Gas-Phase MM2 Association Energies for **10a** and **11a** and Various Encapsulated Guests. $\Delta E_{\text{complex}}$ ^a (kcal/mol)

guest	10a		11a	
	$D^b = 1.0$	4.0	1.0	4.0
naphthalene	-6.0	-4.6	-4.1	-5.3
pyrene	10.5	10.3	12.8	12.8
perylene	19.3	20.4	25.7	24.5
1-DAN	-3.2	2.6	1.8	5.2
α -PNA	2.7 ^c	3.9	5.0	5.1
	5.8 ^d	-0.6		
1-NS	-41.5	-6.0	-47.3	-9.0
ANS	-34.2	3.5	-32.4	4.6
2,7-NDS ^e	-69.3	-16.3	-61.3	14.0
2,6-NDS ^e	-69.9	-11.8	-72.0	-0.9

^a $\Delta E_{\text{complex}} = E(\text{complex}) - E(\text{10a/11a}) - E(\text{guest})$. ^b Dielectric constant. ^c Linear form; see text. ^d Elbow form; see text. ^e The corresponding $D = 1.0$ and 4.0 values for **10b** are -72.5 and -14.0 kcal/mol for 2,7-NDS and -75.0 and -19.4 kcal/mol for 2,6-NDS, respectively.

On the other hand, the noncage host **2** does not exhibit a pH-dependent micropolarity toward these guest molecules. For comparison, the constant E_T^N values for ANS, TNS, and α -PNA are 0.460, 0.707, and 0.386, respectively.

The binding constants (K) of Kyuphane and the noncage host with ANS, TNS, and α -PNA were evaluated on the basis of the Benesi–Hildebrand relationship⁴⁸ for 1:1 host–guest interactions. Good linear correlations of the variation in fluorescence intensity upon addition of the host against the total concentration of the host as judged by double-reciprocal plots^{7b} were obtained at various pH's (Table VII). While the K values for the noncage host **2** with guests are not particularly sensitive to pH attenuation, those for the Kyuphane complexes undergo significant modification over a narrow pH range. Thus, a pH increase from 3.0 to 4.0 results in enhancement of the binding affinity of Kyuphane by 1 order of magnitude toward ANS and TNS, and by 2 orders of magnitude toward α -PNA.

Guest Selectivity. In general, the cationic Kyuphane recognizes guests through hydrophobic and electrostatic interactions similar to the molecular recognition behavior exercised by various cationic cyclophane hosts reported up to the present time. Thus, the present host incorporates nonionic and anionic hydrophobic guests, but not cationic guests such as DASP and safranin O. When we examined the molecular recognition ability of Kyuphane toward various guest molecules in an aqueous acetate buffer at pH 4.0, the following unique complexation behavior was realized as being characteristic of Kyuphane.

(i) Nonionic Guests. We observed size-selective molecular discrimination by Kyuphane toward nonionic fluorescent guests. In order to avoid the possible formation of 1:2 (host to guest) complexes, excess Kyuphane was used for determination of the binding constants on the basis of the Benesi–Hildebrand relationships for the 1:1 host–guest interaction. The binding constants given in Table VIII show that α - and β -PNA fit the host cavity most tightly among the guest molecules examined even though

(47) Reichardt, C. *Solvents and Solvent Effects in Organic Chemistry*; VCH Verlagsgesellschaft: Weinheim, 1988; Chapter 7.

(48) Benesi, H. A.; Hildebrand, J. H. *J. Am. Chem. Soc.* **1949**, *71*, 2703–2707.

pyrene and perylene are more hydrophobic than the PNA's. MM2-optimized host-guest complexes provide qualitative insights into the relative values of the affinity constants.

The force field energy differences between separately optimized hosts and guests and individual complexes for tetracations **10a** and **11a** at dielectric constants of 1.0 and 4.0 ($\Delta E_{\text{complex}}$) are given in Table IX. Were solvent and counterions included, the calculated difference would provide an approximation to the enthalpy of binding. As is, $\Delta E_{\text{complex}}$ is only a rough estimate of ΔH . The ΔS term associated with the experimental K 's can be obtained as a component of a ΔG_{rel} derived by the free energy perturbation technique.⁴⁹ These calculations have not been performed during the course of the present work. Within these limitations, the $\Delta E_{\text{complex}}$'s of Table IX and the associated geometries offer an interesting glimpse into binding properties of the Kyuphane tetracations.

Consider first the simple hydrocarbon series naphthalene, pyrene, and perylene. The first two compounds are bound to the same extent to the host with ΔG 's of -4.8 and -5.2 kcal/mol, respectively, as derived from the K 's of Table VIII. By contrast, the $\Delta E_{\text{complex}}$'s for naphthalene are fortuitously -4 to -6 kcal/mol, while those for pyrene are 10-13 kcal/mol. Inspection of the gas-phase naphthalene complex shows that the geometry of the host is nearly superimposable with that of the uncomplexed tetracation. The 10-carbon aromatic nestles within the cavity ($\bar{V} = 176 \text{ \AA}^3$, Table V) and experiences stabilizing van der Waals interactions. Hosts **10a** and **11a** for pyrene, on the other hand, are modified by torsions around the N-CH₂-Ph bonds and are slightly expanded to accommodate the hydrocarbon. Response to steric compression is evident in the cages' reorganization. Although pyrene sustains $\bar{V} = 251 \text{ \AA}^3$ (Table V), somewhat below the estimated 300- \AA^3 free volume for the cavity, its spatial distribution is not entirely congruent with it. It would appear that the near equality of K 's and ΔG 's for naphthalene and pyrene is a consequence of balanced energy components. Though pyrene is more sterically demanding in the Kyuphane cavity, a hydrophobic effect squeezing the molecule out of the aqueous phase provides the necessary offset.

Perylene's affinity is nearly 1 order of magnitude weaker than pyrene's. The former's increased volume ($\bar{V} = 306 \text{ \AA}^3$) is mirrored in its large and unfavorable calculated $\Delta E_{\text{complex}}$ (19-26 kcal/mol) and in the significant distortions in cage geometry required to accommodate the guest fully in the binding pocket. The point is further amplified by a least-squares fit of the eight nitrogens of the MM2-optimized complexes to the nitrogens of **10a**. The rms deviations for naphthalene, pyrene, and perylene are 0.15, 0.40, and 0.55 \AA , respectively. In the binding event for perylene, hydrophobic forces are less able to override the accompanying deleterious steric effects.

1-(Dimethylamino)naphthalene associates with Kyuphane at pH 4.0 ten times more strongly than naphthalene itself. Although it would be inappropriate to compare the $\Delta E_{\text{complex}}$'s for these two species, the dimethylamino derivative would seem to introduce a new factor. Nearly identical with pyrene in molecular volume ($\bar{V} = 248 \text{ \AA}^3$), the structure likewise promotes moderate torsional rearrangements in the Kyuphane host while exhibiting a 90° rotation around the C(naphthyl)-NMe₂ bond (rms deviation of N's from **10a** 0.33 \AA). In addition, however, the docked aminonaphthalene positions itself such that a N⁺-H of **10a** is oriented to provide a directed electrostatic interaction with the N lone pair (NLP) of the twisted dimethylamino group. The N⁺-H/NLP couple, presumably without a counterpart in solution, may provide the driving force for the increased K relative to naphthalene and pyrene. An additional factor favoring the binding of polar 1-DAN relative to hydrocarbon is its capability of inducing a dipole charge stabilization.

α -PNA is the most tightly held nonionic guest for Kyuphane, 3.3 and 29 times greater than (dimethylamino)naphthalene and naphthalene, respectively. Two conformations were docked into

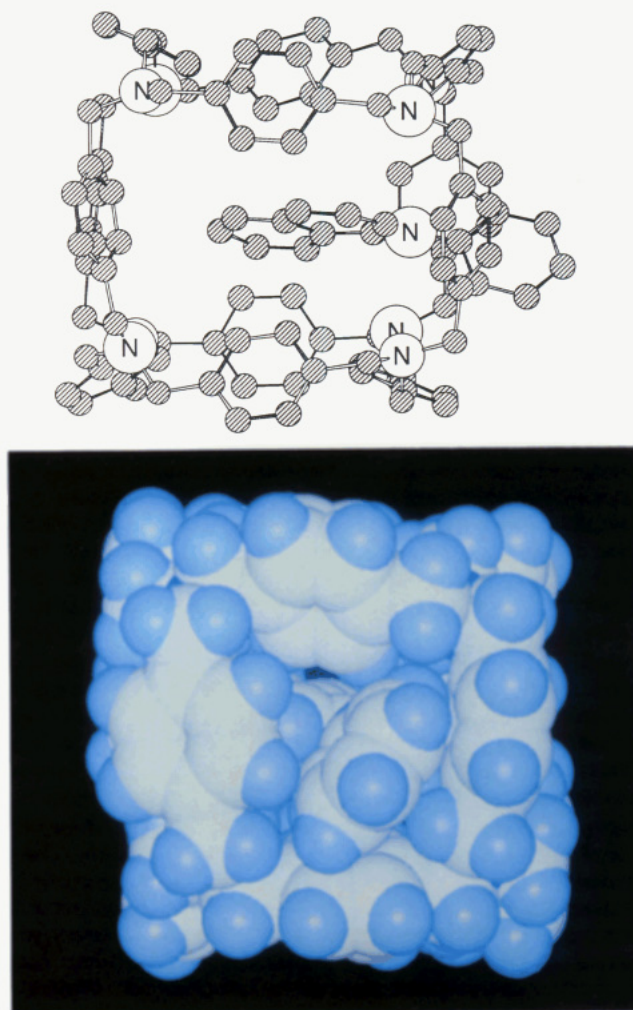


Figure 11. MM2-optimized complex of Kyuphane tetracation **10a** and the linear conformation of α -PNA: (a, top) stick figure; (b, bottom) head-on space-filling model demonstrating the phenyl "plug" in the hydrophobic cage face, SYBYL van der Waals radii.

10a. The "linear" form has the NH-Ph group oriented approximately parallel to the long in-plane naphthalene axis. The "elbow" conformer employs the short axis similarly. The latter is disfavored by 3.1 kcal/mol according to $\Delta E_{\text{complex}}$. In both cases, the NH of the guest is located for productive donor-acceptor interactions with NLP and N⁺-H of the cationic receptor assuming the presence of an intervening water molecule bridge. The relevant N...N and N...H distances range from 3.5 to 4.5 \AA . Furthermore, the terminal phenyls project half to two-thirds of the ring through a Kyuphane face stacking interactions with the four cage phenyls defining the face boundaries are evident. The result is an effective hydrophobic plug blocking solvent entry (Figure 11).

In sum, the binding affinities of nonionic Kyuphane guests are interpretable as a mix of steric effects, electrostatic and hydrogen bonds, hydrophobicity arising from solvent reorganization, and stacking interactions. PNA (α - and β -) appears to have the potential to benefit from all of these. Regardless of the detailed origins of guest selectivity, it can be applied to the selective transport of nonionic molecules between two hexane phases across an aqueous phase containing Kyuphane as a molecular carrier. The transport experiments were performed at 25 °C by utilizing an H-type cell (passage length of the aqueous phase 20 mm) in a manner similar to that reported by Diederich and Dick.⁵⁰ The rate of transport of α -PNA ($4.0 \times 10^{-2} \text{ M}$ in hexane) in 24 h across an aqueous phase containing $1.0 \times 10^{-4} \text{ M}$ Kyuphane at pH 4.0 was 7 times greater than the rate across pure water without

(49) Kollman, P. A.; Merz, K. M. *J. Acc. Chem. Res.* **1990**, 23, 246-252.

(50) Diederich, F.; Dick, K. *J. Am. Chem. Soc.* **1984**, 106, 8024-8036.

Table X. Binding Constants (K) for 1:1 Host–Guest Complexes of Kyuphane (**1**) with Anionic Guests in Aqueous Acetate Buffer (10 mM, μ 0.10 with KCl, pH 4.0) at 30.0 °C

guest	K (M^{-1})	method ^{a,b}
OG	4.4×10^5	A
TNS	4.2×10^5	B
ANS	1.6×10^5	B
5-(dimethylamino)naphthalene-1-sulfonate (5-DA-1-NS)	4.3×10^4	B
naphthalene-2,7-disulfonate (2,7-NDS)	1.4×10^3	C
naphthalene-2,6-disulfonate (2,6-NDS)	1.5×10^2	C
naphthalene-1,5-disulfonate (1,5-NDS)	1.0×10^2	C
naphthalene-2-sulfonate (2-NS)	1.5×10^2	C
naphthalene-1-sulfonate (1-NS)	1.0×10^2	C
(\pm)-10-camphorsulfonate (10-CS)	c	C

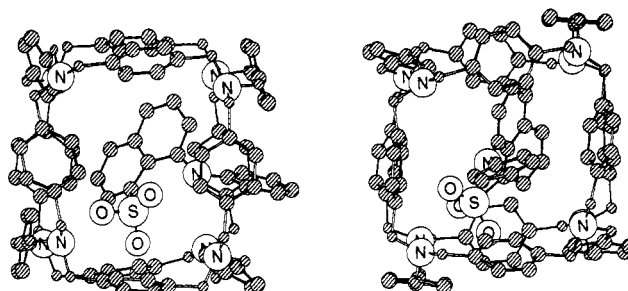
^a Key: A, Benesi–Hildebrand treatment of absorbance data; B, Benesi–Hildebrand treatment of fluorescence data; C, competitive binding against ANS as observed by fluorescence spectroscopy. ^b Method A: OG, 1.0×10^{-5} M; **1**, 3.3×10^{-6} to 2.0×10^{-4} M. Method B: guest, 1.0×10^{-6} M; **1**, 1.0×10^{-5} to 1.0×10^{-4} M. Method C: ANS, 6.67×10^{-7} M; **1**, 6.67×10^{-6} M; guest, 1.33×10^{-6} to 8.00×10^{-6} M. ^c Complex formation was not detected.

Kyuphane. The acceleration factor of 7 for α -PNA is a maximum for the guests employed. The acceleration factors for pyrene, fluoranthene, phenanthrene, acenaphthene, and naphthalene are 1, 2, 2, 1, and 1, respectively.

(ii) **Ionic Guests.** ANS, a naphthalene core complemented by both anilino and sulfonate moieties, binds to Kyuphane at sub-micromolar concentrations (Table X) with a gain in energy of $\Delta G = -7.2$ kcal/mol. Removal of the charged sulfonate group to give α -PNA reduces the binding affinity by 2. In strong contrast, deletion of the anilino functionality to give 1-NS causes a drop in K of 3 orders of magnitude. Similar observations apply to other anionic guests such as TNS and 5-DA-1-NS (Tables VIII and X). In spite of the multiple cationic N^+-H 's directed into the host cavity, loss of anionic sulfonate is 3–4 kcal/mol less costly for complex formation than is loss of neutral NH-Ph.^{51,52} In the present series of guests, hydrophobic effects clearly overwhelm otherwise powerful electrostatic forces. Although the relative calculated binding energies, $\Delta E_{\text{complex}}$ (Table IX), are not meaningful for comparing the structurally diverse TNS, ANS, and 5-DA-1-NS series, the optimized geometries do provide an opportunity for analysis. All calculations were carried out at a dielectric constant of both 1.0 and 4.0, since at the lower value highly charged gas-phase systems frequently experience non-physical structural distortions.

We take ANS as an example. Both linear and elbow forms alone and in the Kyuphane cationic cavity are predicted by MM2 to sustain an intramolecular NH...OS hydrogen bond. The linear conformation in the cavity appears to be considerably more stable. Within **10a**, the NH-Ph group of ANS is situated very similar to that described above for α -PNA (Figure 12). The two NH orientations shadow the potential effectiveness of water-bridged H bonds, while the phenyl ring stacks in the center of a Kyuphane face. In addition, an oxygen of ANS- SO_3^- not involved in intramolecular interaction is Coulombically bonded to a N^+-H in a cage face parallel to that housing the anilino phenyl. The hydrophilic anionic structure 1-NS exhibits an $N^+-H \cdots O^-S$ couple while placing the naphthalene nucleus in the center of the cage. In solution, both ANS and 1-NS undoubtedly promote a highly organized first solvation shell around SO_3^- .

The picture that emerges is one in which host–guest binding capitalizes on hydrophobic events in solution as well as in complex. ANS and α -PNA both bearing a high ratio of nonpolar to polar structure are squeezed out of the aqueous phase as complexation occurs. In addition, the NH-phenyl/cage-phenyl stacking creates an impenetrable boundary that serves to dehydrate at least one

**Figure 12.** MM2-optimized complex of Kyuphane tetracation **10a** and ANS. The NH-Ph projects through the face to the right blocking solvent entry similar to α -PNA, two views.

hydrophobic face. In the process, the ANS- SO_3^- trades its highly favorable aqueous hydrogen-bonding shell for an only slightly more favorable salt bridge. Consequently, ANS and α -PNA differ in binding free energy by the diminutive value $\Delta\Delta G = 0.3$ kcal/mol, though they enjoy K -derived ΔG 's of -7.2 and -6.9 kcal/mol, respectively.⁵¹ On the other hand, 1-NS makes the electrostatic trade with a gain of only -2.8 kcal/mol upon movement from solution to complex, the doubly reinforced hydrophobic effect unavailable to it. A more detailed and quantitative assessment of this analysis is being pursued in the framework of molecular dynamics.^{45,49}

Regioselective molecular discrimination of Kyuphane toward anionic naphthalenedisulfonates, by comparison, operates through the electrostatic host–guest interaction. Although two isomeric species, 1,5-NDS and 2,6-NDS, are recognized by the host with free energy requirements identical with those of the monosulfonates 1-NS and 2-NS, the K value of 2,7-NDS is greater by 1 order of magnitude. Previous considerations based on inspection of space-filling models implied the 2,7-isomer might sustain a better fit than its positional isomers.^{15b} However, comparison of the $\Delta E_{\text{complex}}$'s for the 2,6- and 2,7-variants points to the intervention of several possible Kyuphane forms (Table IX). Guest 2,7-NDS would seem to prefer the tetrahedral cage tetracation (**10b** > **10a** > **11a**), while 2,6-NDS favors the square-planar protonation scheme (**11a** > **10a** > **10b**). Since docking orientations have not been explored comprehensively, this outcome is only suggestive particularly in view of the observation that the binding energy spread between isomers is a diminutive $\Delta\Delta G = 1.4$ kcal/mol.⁵²

What is clear, nonetheless, is that full encapsulation of either 2,6- or 2,7-NDS in the host center is a sterically demanding event. The 278-Å³ volumes of both are near the 300-Å³ limit. In addition, the Kyuphane tetracation is required to expand and reorganize in a manner similar to that of pyrene in the formation of the corresponding complexes (rms deviations of nitrogens relative to **10a** are 0.50 and 0.74 Å at $D = 1.0$ and 0.40 and 0.31 Å at $D = 4.0$, respectively). It would seem that while the doubly charged NDS derivatives benefit from strong in-cage electrostatics, they suffer from complex strain and unfavorable removal from the aqueous phase. The absence of both factors in monosulfonates 1- and 2-NS explains their K equivalence with the naphthalene disulfonates. In turn, this comparison establishes an interpretive basis for the rank order of affinities along the series TNS/ANS > α/β -PNA \approx 5-DA-1-NS > NDS > NS. The complete lack of complexation ability for (\pm)-10-camphorsulfonic acid (10-CS) comes from a different origin. Even though the rigid nearly spherical molecule is just below the allowable molecular volume ($V = 286$ Å³), the small channel in each Kyuphane face prevents the rigid guest molecule from entering the internal cavity as judged from space-filling molecular models of Kyuphane and 10-CS and the dimensions given in Figure 6b.

Molecular Cage Effects. Fluorescence spectral parameters, such as polarization (P), lifetime (τ), and rotational correlation time (θ), originating from guests incorporated into the hosts were evaluated in a manner similar to that reported previously^{7b} (Table XI). Since the microenvironmental polarity experienced by ANS in the host cavity under the present conditions is nearly comparable to that of tetrahydrofuran ($E_T^N = 0.207$), the τ values for the guest

(51) $\Delta G = -RT \ln K$, where $T = 303$ K (Tables VII and VIII).

(52) For example, $\Delta\Delta G(\text{ANS}) = [\Delta G(\text{ANS}) - \Delta G(1\text{-NS})] - [\Delta G(\text{ANS}) - \Delta G(\alpha\text{-PNA})] = \Delta G(\alpha\text{-PNA}) - \Delta G(1\text{-NS}) = 4.1$ kcal/mol. Accordingly, $\Delta\Delta G(\text{TNS}) = 3.7$ and $\Delta\Delta G(5\text{-DA-1-NS}) = 3.3$ kcal/mol.

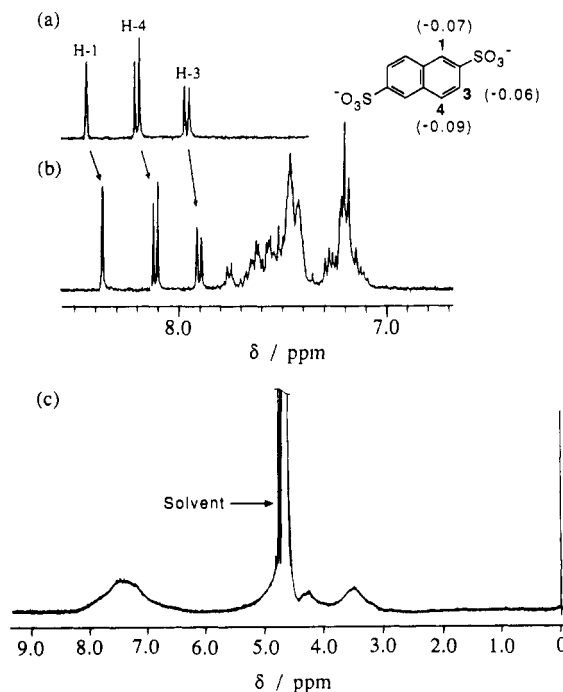
Table XI. Fluorescence Polarization (P), Lifetime (τ), and Rotational Correlation Time (θ), Originating from Guests Incorporated into Azacyclophane Hosts in Aqueous Acetate Buffer (10 mM, μ 0.10 with KCl, pH 4.0) at 30.0 °C under Aerobic Conditions^a

host	guest	P	τ (ns)	θ (ns)
1	ANS	0.24	16.1	17.7
	TNS	0.22	12.2	12.5
2	ANS	0.12	10.7	4.16
	TNS	0.19	9.95	7.57

^a Concentrations: guests, 1.0×10^{-6} M; hosts, 1.0×10^{-5} M.

were also measured in the same organic solvent: 9.2 and 16.0 ns under aerobic and anaerobic conditions, respectively. This implies that the molecular cage of Kyuphane completely protects the incorporated guest from oxygen attack. A similar cage effect was also seen for TNS. The τ values are 8.4 and 11.9 ns under aerobic and anaerobic conditions, respectively, in ethanol ($E_T^N = 0.654$). The polarity of ethanol is equivalent to the micropolarity experienced by TNS in the host cavity. In addition, the θ values for guests bound to Kyuphane are significantly large even though they are somewhat smaller than that found for ANS bound to the octopus cyclophane ($\theta = 23$ ns).^{7b} High microscopic viscosity in the hydrophobic cavity of the host is indicated. In contrast, all the fluorescence spectral parameters for guests incorporated into **2** are much smaller relative to the corresponding values observed by complexation with **1** (Table XI).

We also investigated the host-guest interactions of Kyuphane and the noncage host **2** with various hydrophobic guests by means of ¹H NMR spectroscopy. With naphthalene-2,6-disulfonate as a guest molecule, the noncage host demonstrated normal complexation behavior as shown in Figure 13. Proton signals for the guest shifted upfield upon complexation in a manner previously observed for various host-guest systems. On the other hand, proton signals for the guest molecule completely disappeared upon complexation with Kyuphane, and only the proton signals for Kyuphane remained (Figure 13c). In this case, the $\Delta\nu_{1/2}$ value for the aromatic proton signals were broadened from 213 to 287 Hz while the methylene proton signals were converted from a broad singlet to two broad singlets upon complexation. The latter spectral behavior indicates that four of the eight protonated amino nitrogens present in cage **1** at pH 2.4 have been deprotonated through interaction with the included guest. Similar disappearance of proton signals was also noticed for other anionic guests, such as ANS and TNS, upon complexation with Kyuphane. Nevertheless, proton signals for guests, which do not form complexes with Kyuphane due to electrostatic repulsion, such as safranin O, or due to excessive bulkiness, such as (\pm)-10-camphorsulfonate, were not affected at all in the presence of Kyuphane. Thus, the disappearance of guest signals upon complex formation is a specific feature characteristic of Kyuphane. It can be explained as follows. Since intramolecular rotation of the eight phenyl groups of Kyuphane is extremely sluggish even in solution as indicated by the broad ¹H NMR signals, protons of a guest molecule placed in the host cavity are subjected to complicated anisotropy effects exerted by the multiple phenyl rings of the host molecule. At the same time, the molecular motion of a guest molecule incorporated into the host cavity would seem to be severely restricted as indicated by the θ parameters for ANS and TNS (Table XI). In this circumstance, proton signals for the guest are subjected to extreme line broadening so as to disappear. Alternatively, if the

**Figure 13.** ¹H NMR spectra in D₂O at 30.0 °C with TSP as an external reference: (a), [naphthalene-2,6-disulfonate] = 1.2 mM at pD 1.2; (b), [2] = [naphthalene-2,6-disulfonate] = 0.12 mM at pD 1.2; (c), [1] = [naphthalene-2,6-disulfonate] = 0.12 mM at pD 2.4.

difference in NMR correlation times between host and guest are great, reflecting a relative tumbling of guest inside host, the result recorded by Figure 13c can be the outcome. While TNS and ANS do not seem to fulfill this requirement, smaller molecules such as 2,6-NDS may do so. This question is under investigation in our laboratories.

Concluding Remarks

A novel host, Kyuphane, was designed and synthesized as the structural fusion of semirigid azacyclophane skeletons. Its molecular recognition ability as a tetracation has been clarified in aqueous media. The constrained but mobile hydrophobic internal cavity provided by Kyuphane is suitable for molecular recognition through the biomimetic lock-and-key mechanism. Several structural features characteristic of Kyuphane, which originate from its unique molecular structure, are now apparent. The versatile molecular cage is expected to be utilized as an artificial carrier, enzyme, or receptor.

Acknowledgment. We are grateful to Professor Takahiko Inazu of Kyushu University for his kind comments on the synthetic manipulation of compound **3**, and to Professor Masashi Tashiro of Kyushu University and Professor Kazunori Sakata of Kyushu Institute of Technology for mass spectroscopic measurements. Dr. Michael Connolly generously provided access to the molecular volume estimation routines. We are likewise appreciative of Dr. Dale Spangler, Dr. T. J. O'Donnell, and Gregory Tipword (Searle) for programming assistance. This work was supported by a Grant-in-Aid for Scientific Research No. 01470097 and a Special Distinguished Grant for Scientific Research No. 02102006 from the Ministry of Education, Science, and Culture of Japan.